HAROKOPIO UNIVERSITY

School of Environment, Geography and Applied Economics
Department of Geography
Postgraduate Program of Applied Geography and Spatial Planning – Geoinformatics

A GEOBIA-based approach for mapping Urban Green Spaces using PlanetScope and Sentinel-2 imagery: the case of Athens

Master Thesis

Evangelos Dosiadis

Athens, 2022

ΧΑΡΟΚΟΠΕΙΟ ΠΑΝΕΠΙΣΤΗΜΙΟ

Σχολή Περιβάλλοντος, Γεωγραφίας και Εφαρμοσμένων Οικονομικών
Τμήμα Γεωγραφίας
Πρόγραμμα Μεταπτυχιακών Σπουδών Εφαρμοσμένη Γεωγραφία και Διαχείριση του Χώρου
Κατεύθυνση Γεωπληροφορικής

Χαρτογράφηση Αστικού Πρασίνου με τη χρήση αντικειμενοστραφούς ταξινόμησης σε δορυφορικές εικόνες PlanetScope και Sentinel-2: η περίπτωση της Αθήνας

Μεταπτυχιακή εργασία

Ευάγγελος Δοσιάδης

Αθήνα, 2022

HAROKOPIO UNIVERSITY

School of Environment, Geography and Applied Economics
Department of Geography
Postgraduate Program of Applied Geography and Spatial Planning –
Geoinformatics

Supervisor

George P. Petropoulos
Assistant Professor, Department of Geography, Harokopio University

Committee

Issaak Parcharidis
Professor, Department of Geography, Harokopio University

Dionysios Kalyvas
Associate Professor, Department of Natural Resources Development and
Agricultural Engineering, Agricultural University of Athens

Ethics and Copyright Statement

I, Evangelos Dosiadis, hereby declare that:

1) I am the owner of the intellectual rights of this original work and to the best of my knowledge, my work does not insult persons, nor does it offend the intellectual rights of third parties.

2) I accept that the Library and Information Centre of Harokopio University may, without changing the content of my work, make it available in electronic form through its Digital Library, copy it in any medium and/or any format, and hold more than one copy for maintenance and safety purposes.

3) I have obtained, where necessary, permission from the copyright owners to use any third-party copyright material reproduced in the master thesis while the corresponding material is visible in the submitted work.

Acknowledgments

I would like to express my sincere gratitude to my supervisor Dr. Georgios P. Petropoulos for his unlimited guidance and feedback throughout all the steps of the present thesis. He has consistently given me opportunities to acquire new skills, knowledge, and experience.

I also wish to thank my family and my friends for their support throughout all the years of my tertiary studies.

Hereby I would also like to mention that part of this work has already been presented at the European Geosciences Union General Assembly 2022 (Dosiadis et al., 2022a). Part of it has also been published as a chapter in the book "Earth Observation in Urban Monitoring: Techniques and Challenges" (Dosiadis et al., 2022b).

Abstract

The technological developments in geoinformatics in recent decades have allowed the inclusion of geospatial data and analysis techniques in a wide range of scientific disciplines. One such field is the study of urban green spaces, which are open, undeveloped areas that provide residents with recreational space, while at the same time they help to improve the aesthetic and environmental quality of the neighboring areas. They form an ecosystem, which provides the society with services that may be cultural, provisioning or regulating, and managing. The evaluation and assessment of the urban green spaces are very important in order for them to be identified, monitored, and optimized.

The objective of the present thesis is to map the urban green spaces in the city of Athens using high spatial-resolution satellite imagery of 3 meters from PlanetScope and medium spatial-resolution imagery of 10 meters from Sentinel-2. The retrieval of the urban green spaces is conducted in ArcGIS Pro using the Geographic Object-Based Image Analysis (GEOBIA) classification method, by which the study area is segmented into polygons according to the spectral resolution of the image's pixels. Then, the Random Trees and Support Vector Machines (SVM) classifiers are utilized for the classification of the images, trained by a collection of samples generated by the segmentation. The validation approach is based on the confusion matrix using accuracy assessment points as reference and on the comparison of the extracted green areas with the Urban Atlas.

The results revealed a high Overall Accuracy of above 90% and K_c values between 0.83 and 0.9 for both imagery and both classifiers. The PlanetScope imagery resulted in higher accuracy on both classifiers in comparison with the Sentinel-2 imagery proving that high resolution works better in urban areas. On the same note, the Random Trees classifier provided higher accuracy on both imageries in comparison with the SVM. The extracted green areas' comparison to the Urban Atlas resulted in large differences making it unsuitable as validation data.

The methodology implemented in this thesis and the key study findings may provide an important contribution toward the implementation of successful urban landscape planning and infrastructure development in Athens. Further study could be focused on determining the species and health of the vegetation and the quality of the ecosystem services provided by the city's green areas.

Keywords: Urban Green Spaces · GEOBIA · Remote Sensing · PlanetScope · Sentinel-2 · Classification · Athens

Περίληψη

Οι τεχνολογικές εξελίξεις τις τελευταίες δεκαετίες στον τομέα της γεωπληροφορικής έχουν επιτρέψει τη συμπερίληψη γεωχωρικών δεδομένων και τεχνικών ανάλυσης σε ένα ευρύ φάσμα επιστημονικών κλάδων. Ένας τέτοιος τομέας είναι η μελέτη των αστικών χώρων πρασίνου, οι οποίοι είναι ανοιχτοί, μη ανεπτυγμένοι χώροι που παρέχουν στους κατοίκους χώρους αναψυχής, ενώ παράλληλα συμβάλλουν στη βελτίωση της αισθητικής και περιβαλλοντικής ποιότητας των όμορων περιοχών. Αποτελούν ένα οικοσύστημα, το οποίο παρέχει στην κοινωνία υπηρεσίες που μπορεί να είναι πολιτιστικές, προμηθευτικές ή ρυθμιστικές και διαχειριστικές. Η αξιολόγηση των χώρων αστικού πρασίνου είναι πολύ σημαντική για τον εντοπισμό, την παρακολούθηση και τη βελτιστοποίησή τους.

Στόχος της παρούσας διπλωματικής εργασίας είναι η χαρτογράφηση των χώρων αστικού πρασίνου στην πόλη της Αθήνας χρησιμοποιώντας δορυφορικές εικόνες υψηλής χωρικής ανάλυσης 3 μέτρων από το PlanetScope και εικόνες μέσης χωρικής ανάλυσης 10 μέτρων από το Sentinel-2. Η ανάκτηση των χώρων αστικού πρασίνου πραγματοποιείται στο ArcGIS Pro χρησιμοποιώντας τη μέθοδο ταξινόμησης Geographic Object-Based Image Analysis (GEOBIA), με την οποία η περιοχή μελέτης τμηματοποιείται σε πολύγωνα σύμφωνα με τη φασματική ανάλυση των ψηφίδων της εικόνας. Στη συνέχεια, οι ταξινομητές Random Trees και SVM χρησιμοποιούνται για την ταξινόμηση των εικόνων, εκπαιδευμένοι από μια συλλογή δειγμάτων που δημιουργούνται μέσω του επιπέδου της τμηματοποιημένης εικόνας. Η επικύρωση των αποτελεσμάτων βασίζεται στον πίνακα σύγχυσης χρησιμοποιώντας σημεία αξιολόγησης ακρίβειας ως αναφορά και στη σύγκριση των εξαγμένων περιοχών πρασίνου με το Urban Atlas.

Τα αποτελέσματα αποκαλύπτουν υψηλή συνολική ακρίβεια (OA) άνω του 90% και τιμές του δείκτη K_c μεταξύ 0,83 και 0,9 τόσο για τις εικόνες όσο και για τους δύο ταξινομητές. Οι εικόνες του PlanetScope σημείωσαν υψηλότερη ακρίβεια και στους δύο ταξινομητές σε σύγκριση με τις εικόνες Sentinel-2, αποδεικνύοντας ότι η υψηλή χωρική ανάλυση λειτουργεί καλύτερα σε αστικές περιοχές. Παράλληλα, ο ταξινομητής Random Trees παρείχε υψηλότερη ακρίβεια και στις δύο εικόνες, σε σχέση με το SVM. Η σύγκριση των εξαγόμενων χώρων πρασίνου με το Urban Atlas οδήγησε σε μεγάλες διαφορές που τον καθιστούν ακατάλληλο ως δεδομένα επικύρωσης.

Η μεθοδολογία που χρησιμοποιήθηκε σε αυτή τη διπλωματική και η θετική εικόνα των αποτελεσμάτων μπορούν να συμβάλουν σημαντικά στην υλοποίηση ενός επιτυχημένου σχεδιασμού αστικού τοπίου και ανάπτυξης πράσινων υποδομών στην Αθήνα. Περαιτέρω μελέτη θα ήταν επιθυμητό να πραγματοποιηθεί σε σχέση με τον προσδιορισμό του είδους και της υγείας της βλάστησης και της ποιότητας των οικοσυστημικών υπηρεσιών που παρέχονται από τις περιοχές πρασίνου της πόλης.

Λέξεις κλειδιά: Αστικοί Χώροι Πρασίνου · GEOBIA · Τηλεπισκόπηση · PlanetScope · Sentinel-2 · Ταξινόμηση · Αθήνα

Contents

List of figures

List of tables

List of abbreviations

ANN	Artificial Neural Network
CICES	Common International Classification of Ecosystem Services
CNN	Convolutional Neural Network
EO	Earth Observation
ESA	European Space Agency
FUA	Functional Urban Areas
GEE	Google Earth Engine
GEOBIA	Geographic Object-Based Image Analysis
GIS	Geographic Information Systems
GLCM	Gray-Level Co-occurrence Matrix
GMES	Global Monitoring for Environment and Security
GMS	Global Monitoring for Environment and Security
GUA	Green Urban Areas
HNMS	Hellenic National Meteorological Service
HSR	High-Spatial Resolution
KNN	K Nearest Neighbor
L1C	Level-1C
L2A	Level-2A
LULC	Land Use/Land Cover
MA	Millennium Ecosystem Assessment
MSI	Multi-Spectral Instrument
NDVI	Normalized Difference Vegetation Index
NDWI	Normalized Difference Water Index
NIR	Near Infrared
OA	Overall Accuracy
OBIA	Object-Based Image Analysis
OOB	Out-Of-Bag
RF	Random Forest
RGB	Red, Green, Blue
S2A	Sentinel-2A
SVM	Support Vector Machine
SWIR	Short Wave Infrared
TEEB	The Economics of Ecosystems and Biodiversity
UAV	Unmanned Aerial Vehicle
UGS	Urban Green Space
UN	United Nations
VHR	Very-High Resolution
WHO	World Health Organization
WWF	World Wide Fund

Chapter 1: Introduction

1.1. Preamble

Urban Green Spaces are open, non-developed urban areas covered by vegetation that include parks, road green spaces, residential green spaces, river banks, and urban forests (Huerta et al., 2021; Petropoulos et al., 2013a; Petropoulos et al., 2015). UGSs are of great importance for the urban natural environment, public health and urban planning. The ecosystem services provided by the UGSs have various positive impacts of crucial importance. They enhance the urban area's environmental quality by managing microclimate and decreasing the heat island effect, while at the same time contributing to lowering atmospheric carbon dioxide, eliminating air pollutants, and promoting biodiversity (Lau et al., 2021; Javadi & Nasrollahi, 2021). Furthermore, UGSs facilitate physical activity and social interactions, and reduce mental stress, improving the physical and mental health of urban residents (Dadvand et al., 2016; Jennings & Bamkole, 2019). Therefore, UGSs contribute to direct and indirect benefits for the well-being and overall quality of life of the urban population. However, the constant expansion of urbanization trends in recent decades has provoked loss and degradation in green spaces, especially those within or in immediate proximity to urban centers (Scott et al., 2014; Puplampu & Boafo, 2021; Noszczyk et al., 2022). As noted by the United Nations, in 2017 more than half the world population (55%) lived in urban areas, while the ratio is estimated to reach 68% by 2050. Hence, UGSs are progressively viewed as essential aspects of urban planning, and their preservation and expansion in Metropolitan areas are of high importance to protect the environment and people's health (Cheng et al., 2021; Liu et al., 2022).

With the evolution of geoinformation, the study of UGSs mapping has been optimized and facilitated, leaving aside conventional methods, like field survey and ground-data-collection techniques that are time-consuming and cost-ineffective (Pandey et al., 2019; Timilsina et al., 2020). Geoinformation technologies such as Geographical Information Systems (GIS) and Earth Observation (EO) provide an avenue that is very promising towards obtaining a cartography of the UGSs and of their changes over time. This is due to the number of advantages offered by EO, including the inexpensive data acquisition and analysis, and the availability of synoptic views at different geographical scales (Elatawneh et al., 2012; Petropoulos et al., 2013b; Li et al., 2014; Whyte et al., 2018). Furthermore, the integration of GIS offers a set of geospatial data analysis tools that can support a rapid and cost-effective development of solutions for data storage, capture, synthesis and analysis of information spatially, providing additional help to support urban planning and decision making (Dawson et al., 2019; Fragou et al., 2020).

Imagery from EO sensors acquiring data at medium or coarse resolutions is not the optimum solution in UGSs studies as the acquisition of such data does not have the spatial information required to discern fragmented vegetation cover. Aerial images have also not been widely employed in urban studies due to their restricted coverage of a scene, considerable intervals between revisits, and high cost. In recent years, EO technology has rapidly evolved from a technological point of view as evidenced by the launch of new EO imagine sensors able to provide information from space at very high spatio-temporal resolutions (Petropoulos et al., 2012a; Cass et al., 2019). As such, the preferred option in mapping UGSs is the use of very high resolution (VHR) imagery from satellite sensors such as IKONOS, QuickBird, and PlanetScope.

UGS mapping can be conducted using a variety of approaches based mainly on classification, including pixel-based and object-based techniques (Lu & Weng, 2007; Wulder et al., 2018). Pixel-based techniques utilize information acquired in the reflective part of the electromagnetic spectrum, and this information is used in a classification scheme to assign pixels to land cover classes including UGS. Most commonly, those classifiers employ "training sites," which are samples of a given identity for each land cover class, to classify image pixels of unknown identity (Churches et al., 2014). Among the most commonly used pixel-based classifiers are Random Forest (RF), Decision Tree, Artificial Fuzzy-set CTA Algorithm, Artificial Neural Network (ANN), k-Nearest Neighbor (KNN), SVM, and Expert Systems (Al-Doski et al., 2020). On the other hand, in object-based (GEOBIA) classification the basic processing units are image objects or segments, and not single pixels (Petropoulos et al., 2012b; Zhou et al., 2014; Cass et al., 2019). The representation of image information by objects directly connects these objects within a topological network, allowing the efficient use of many different kinds of relational information. Object-based techniques focus on the aggregation of the pixels of the image in homogenous regions-objects based on their spectral, spatial, and contextual properties, contrary to the pixel-based approach that classifies individual pixels directly (Puissant et al., 2014; Gülçin & Akpınar, 2018; Pandey et al., 2020). In recent years, object-based image analysis has been gaining ground as high and very high-resolution (VHR) satellite images are becoming more easily accessible (Hossain & Chen, 2019). However, VHR satellite images don't perform very well when applying conventional pixel-based classification techniques particularly so in areas or targets having complex spatial structures and similar spectral characteristics among urban vegetation categories. Therefore, the combination of GEOBIA with VHR satellite images in the classification process allows for maximizing the amount of information on spatial neighborhood properties available in EO imagery. As such, this approach allows depicting in a much more realistic way the true spatial patterns that exist in an imagery, in comparison to a pixel-based classifier that treats an EO image as a uniform pixel (Pandey et al., 2020).

1.2. Aims and objectives

In purview of the above, the present study aims at exploring the use of the high and medium spatial resolution satellite imagery from PlanetScope and the medium spatial resolution satellite imagery from Sentinel-2, combined with the Geographic Object-Based Image Analysis (GEOBIA) classification approach and the Random Trees and SVM classifiers in mapping urban green spaces (UGSs) for the metropolitan city and capital of Greece, Athens.

With respect to the above, this thesis aims to map the urban green spaces in the Greater Athens Area, Greece. This aim is based on two main objectives, as presented below:

i) Utilization of an object-based approach with the SVM and Random Trees classifiers for mapping UGSs with high-resolution PlanetScope imagery
ii) Using the same object-based approach with the SVM and Random Trees classifiers for mapping UGSs with medium-resolution Sentinel-2 imagery

The comparison of the two imagery datasets and the two classifiers aims to facilitate the determination of which is more appropriate for the study of green spaces in densely built-up urban areas.

1.3. Thesis structure

The present thesis consists of eight chapters. Chapter 1 introduces the research topic, the urban green spaces, and the remote sensing techniques and data used for mapping the UGSs. Chapter 2 discusses the literature review that is related to the present thesis. In particular, it provides the importance of the UGSs for the overall quality of life in the cities that is provided to the residents and visitors by their ecosystem services. Additionally, it describes the groups of methods based on remote sensing data that are used in UGSs mapping. Chapter 3 includes an overview of information about the study area. Chapter 4 outlines the datasets used for mapping the UGSs in Athens. Chapter 5 describes the methodology explaining the steps followed for the classification of the imagery and the extraction of the UGSs, as well as the validation of the method. Chapter 6 is the results section where the analysis findings are presented in maps and statistics tables. Chapter 7 is the discussion section where the strengths and weaknesses of the analysis are identified from the results and are linked to the literature. Chapter 8 is the final chapter of the conclusions which summarizes the overall findings of the thesis and mentions the limitations of the methods as well as its future perspectives.

Chapter 2: Literature review

This chapter aims at presenting the importance of the UGSs mapping and an overview of the literature surrounding the main groups of analysis techniques and methods used for the accomplishment of this purpose, as well as of the relevant operational products available.

2.1. Urban Green Spaces

UGSs refer to non-developed public and private areas within the urban fabric that include vegetated natural and semi-natural areas such as parks, gardens, river beds, roundabouts, green roofs, airfields, golf courses, and other green areas (Reyes-Riveros et al., 2021). The importance of UGSs mapping lies in the ecosystem services linked to the green spaces and the benefits that the natural environment provides people with, either directly or indirectly (Pinto et al., 2021). The term “ecosystem services” was first coined in 1981 and became widely used during the 1990s, initially focusing on their economical values and later showing equal importance to the ecological values as well (Burkhard & Maes, 2017).

The ecosystem services are generally classified into three main systems: provisioning, regulating, and cultural services. There are three international classification systems (MA, TEEB, CICES) that base their classification on the aforementioned classes, each with its own advantages and disadvantages. The Millennium Ecosystem Assessment (MEA, 2005) was the initial proposed classification on which the other two are based, and it includes four groups of services: i) Provisioning, ii) Regulating, iii) Cultural, and iv) Supporting (MEA, 2005). The Economics of Ecosystems and Biodiversity (TEEB) largely follows the MA, with the substitution of supporting services for habitat services. This alteration is adopted as the former is viewed as a subset of ecological processes, while the latter is considered a provider of habitat for migratory species and protection for the species gene pool. The service classes that immerge from the TEEB are as follows: i) Provisioning, ii) Regulating, iii) Habitat, iv) Cultural and amenity (Kumar, 2011). The Common International Classification of Ecosystem Services (CICES) focuses on the way living systems give rise to the ecosystem services and further classifies the three major classes of i) provisioning, ii) regulating and maintenance and iii) cultural in biotic and abiotic (Haines-Young & Potschin-Young, 2018).

According to Ferreira et al. (2022), ecosystem services provide benefits that can be divided into 3 levels; the ecological level, the social level, and the economic level. At the ecological level, the benefits are concentrated on the biodiversity of the area concerned and the contribution to better air quality through the absorption of pollutants and the reduction of the particulate matter concentration, as well as mitigating noise pollution. Additionally, they regulate the air temperature helping reduce the heat island effect, and mitigate the risk of flooding and erosion. At the social level, they provide space for social interaction and recreational activities, encouraging people to socialize and engage in physical exercise, resulting in reducing stress and obesity, overall improving the residents’ well-being. At the economic level, the benefits can be direct and indirect. The direct benefits are related to the activities that derive from the UGSs, the enhancement of the commercial areas’ quality, and the promotion of tourism thanks to their attractiveness. The indirect benefits are linked to the former two levels. The overall ecological regulation and its effects on the cities’ microclimate save energy consumption and production. On the same note, social interaction reduces the medical care and increases the residents’ productivity by improving their mental and physical health.

Urban areas are home to 55% of the human population, predicted to increase to 2/3 by 2050 according to the United Nations (2018). Their densification provides housing for more people but at the same time reduces the natural environment (Sharifi et al., 2021). It is generally accepted that these urbanization trends deteriorate the development and preservation of ecosystem services, though, there are cases where the opposite happens, like in arid and semi-arid areas as a result of irrigation (Wang et al., 2019). Most countries around the world face a lack of data and records on ever-changing land use in urban areas that fragments and degrades the UGSs. The authorities tend to refer to outdated sources for planning and managing the UGSs, therefore posing a hindrance in the decision-making process and rendering the creation of detailed mapping a necessity (Lahoti et al., 2019). The quantification of the urban green patterns and their spatiotemporal changes caused by urban expansion is facilitated by modern remote sensing techniques that provide more accurate and reliable results (Colding et al., 2020). UGSs mapping helps in decision-making that ensures that the environmental quality of the cities remains or reaches high standards (Degerickx et al., 2020).

The information of UGSs, typically presented in the form of a shapefile, is not updated frequently and, as a result, the spatiotemporal changes are not presented. At the same time, the United Nations has stressed the lack of availability of the UGSs data to the public and the necessity for their improvement and free distribution for the creation of more sustainable cities (Huerta et al., 2021). Green spaces are a vital ecological instrument that has the means to improve public health. Since its expansion is somewhat troublesome to be realized in many cases, at the very least the local authorities need to ensure its quality (Ghahramani et al., 2021).

2.2. Overview of EO and GIS-based data and methods

This section covers a review of the methods and thematic applications for Urban Green Spaces mapping with the use of Earth Observation (EO) data and/or GIS-related software. The whole section is based mostly on two review papers that focus explicitly on this topic, Neyns and Caters (2022) and Shahtahmassebi et al. (2021).

The study of green spaces in urban areas was centered around the visual interpretation of aerial photos and fieldwork before 2000, due to the lack of the necessary technology for remote sensing and image processing techniques. A trend of a rapid increase in the use of remote sensing was observed thereafter, with increased availability of remote sensing technology in terms of different satellites and spatial resolution. Additionally, the introduction of LiDAR and hyperspectral sensors have facilitated the generation of information on the vertical structure of the plants and the identification of different plant species. A further boost in the use of satellite imagery was given by the free accessibility of LANDSAT data after 2009 and the implementation of the Copernicus program by the European Space Agency with free and open access data in 2015. International organizations, such as the World Health Organization (WHO), have suggested the demand for extending the investigation of UGSs via remote sensing analysis, showing the increasing need for their monitoring.

According to Kartalis and Feidas (2012), remote sensing is used to describe the process of obtaining information about an object, area, or phenomenon using detection devices that are not in contact with the object of observation. Although the term of remote sensing can be used for any remote sensing action, has been established for the recording and analysis of satellite imagery. A satellite refers to an object or body moving around another body. It focuses, however, primarily on artificial satellites orbiting the earth and used in telecommunications and observation (Perakis, 2015).

The use of remote sensing for studying UGSs includes several factors that are taken into consideration by the authors, namely the thematic area of each study, the spatial and spectral resolution of the imagery, the image's timing acquisition, and the user demands and cost-efficiency. The scale of the study area and the specific purpose of the study determine the spatial and spectral resolution of the required imagery, with more studies opting for medium spatial resolution and multispectral sensors, as they are freely accessible. Though the high spatial resolution is ideal for combusted urban areas, it may also lead to drawbacks, such as low within and between-class variability and the effect of shadow which reduces classification accuracy, as well as the cost factor which may increase significantly. Hyperspectral imagery, due to its limited accessibility, is observed in a very small portion of the studies and it is usually preferred in cases of identifying vegetation species. Regarding the timing acquisition, it is suggested that the imagery is chosen during the peak of the phenological cycle, which depending on location is in late spring. However, when the study involves the distinction between plant species, a way to avoid the discrimination caused by their respective phenological cycle is to combine multi-date imagery.

Geographic Information Systems (GIS) are one of the most important branches of Geoinformatics and thus have been established worldwide over the last three decades in the study of objects, phenomena, and natural processes that have a spatial dimension (Pappas, 2017). Their use is crucial in the applications of multidimensional actions and services that contribute to a large part of people's daily lives, from the appropriate spatial positioning of mobile phone antennas to the construction of maps for the study of natural phenomena and disasters (Chalkias, 2015). GIS software have been used only by a small fraction of the revised papers on UGSs mapping, where ESRI's ArcGIS Desktop was preferred among the existing software (Kopecká et al., 2017; Lahoti et al., 2019).

2.2.1. Analytical techniques for UGSs mapping

The analysis of the UGSs mapping in the literature is based on 5 major techniques, determined by each study's thematic area; hybrid methods; object-based techniques; land cover indices; fraction methods; pixel-based techniques **(Figure 2.1.)**. The most often used technique is the hybrid method which has been used by 29% of the examined papers. Its advantage lies in the combination of different algorithms in one framework in order to increase the performance, most notably by combining pixel-based with object-based methods and soft classifiers. Its disadvantages depend on the individual study and the combination of methods.

Second in frequency are the object-based techniques (OBIA), which have been used by 22.8% of the papers. They are the most common in imagery with high spatial resolution and are based on segmentation algorithms that are mainly performed in the eCognition software. According to the Strengths, Weaknesses Opportunities and Threats (SWOT) analysis performed by Hay & Castilla (2008), the technique's main strengths are related to the partition of the image into objects which are more comprehensible for the human conceptual understanding. Additionally, the objects reduce the computational classifier loads and allow for the use of more complete techniques. They also include useful features, such as shape and texture, and they are easier to integrate into a vector GIS. On the other hand, the weaknesses lie in the complicated nature of segmentation and its parametrizations.

Land cover indices come next with 20 appearances (15.8%) and usually combine the wave bands of the multispectral sensors in order to create indices. One such index is the Normalized Difference Vegetation Index (NDVI), derived from the red and Near Infrared (NIR) bands and used for locating live green vegetation (Chen et al., 2017). They are preferred by many authors thanks to their simplicity in terms of interpretation, as well as to their continuous spatial variable that can be integrated into modeling and simulations. Their limitations are concentrated mostly in the saturation that is caused when the study area is covered by high canopy and leaf area index (Lu et al., 2017).

Fraction methods (16 appearances) work at the subpixel level and they are especially effective when applied to imagery of medium spatial resolution. The effect of endmember spectral variability is one of the methods' disadvantages that needs to be overcome for the analysis to conclude to more accurate results (Shao & Lan, 2019).

Finally, pixel-based analysis had been the traditional classification technique for years but has been progressively replaced by the methods mentioned above, with only 11 papers performing this method. It can be divided into unsupervised and supervised classification. The unsupervised classification divides a remote sensing image into several classes defined by the user, based on the image values without previous knowledge about the study area or training data. The supervised classification is performed with the use of training samples that are selected based on the spectral properties of the pixels (Li et al, 2014). In essence, in this type of analysis, each image pixel is analyzed based on the spectral information it contains. This poses its fundamental limitation, as classes that show high spectral heterogeneity are likely to be labeled as different classes, creating the salt-and-pepper effect. This effect is especially profound in highly heterogeneous landscapes like urban areas (Shahtahmassebi et al., 2021).

Table 2.1.
Main advantages and disadvantages of the main groups of methods used for remote sensing image classification (Hay & Castilla, 2008; Li et al., 2014; Lu et al., 2017; Chen et al., 2017; Shao & Lan, 2019; Shahtahmassebi et al., 2021)

Classification methods	Advantages	Disadvantages
Hybrid	combination of different techniques - increased performance	variation depending on the combination of methods
Object-based	objects are more comprehensible to the human eye objects reduce computational errors information on object's spatial, textural, and contextual properties	segmentation may be a complicated process
Land cover indices	simplicity in interpretation	possible image saturation
Fraction	consideration of each pixel's spectral variability	endmember spectral variability
Pixel-based	simplicity in execution	within-class spectral variation salt and pepper effect

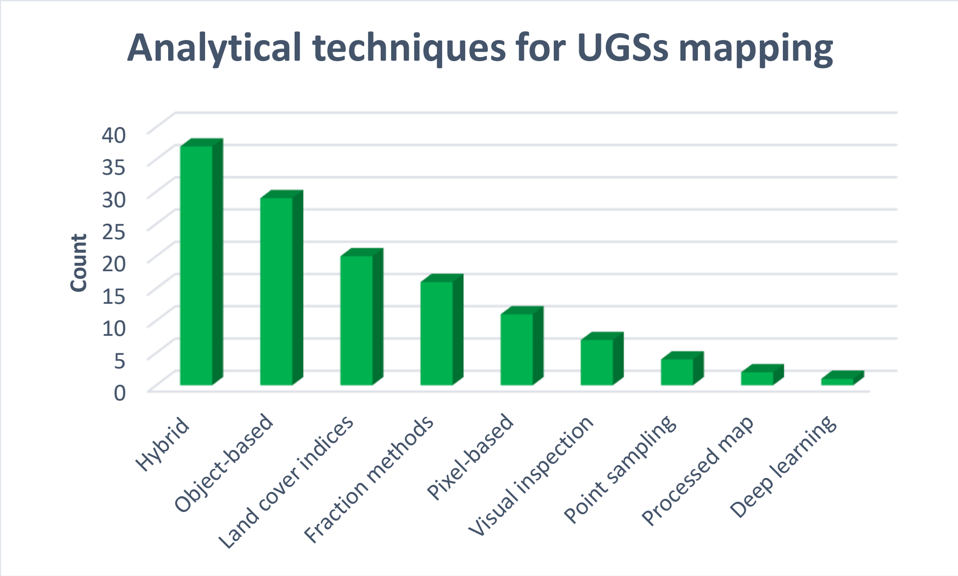

Figure 2.1. Graph depicting the analytical techniques for Urban Green Spaces mapping and their frequency of appearance in the literature based on the review paper by Shahtahmassebi et al. (2021)

2.2.2. Classification approaches for UGSs

There are various classification approaches that are used to map urban vegetation **(Table 2.2.; Figure 2.2.)**. The most popular of them are the supervised learning approaches which can be divided into parametric and non-parametric methods. The parametric classifiers are easy to process and interpret, though they result in lower performance due to the invalidity of the assumptions that are made on the distribution of the data. The most common parametric classifier in the studies regarding UGSs is the Maximum Likelihood (Neyns & Caters, 2022). On the other hand, non-parametric classifiers are more widely used, including the Support Vector Machine, Decision Tree, and Random Forest, with the latter being the most popular classifier for UGSs mapping. The library-based classification is used by several authors, where endmember signatures are utilized to map the vegetation at the pixel or sub-pixel level with the spectral mixture analysis or the algorithm of the spectral angle mapper (Neyns & Caters, 2022). Finally, deep learning is a classification technique that covers various neural network architectures and is used in either supervised, unsupervised or semi-supervised learning. Three deep learning algorithms that have been used in mapping urban green spaces are the Boltzman machine, the MLP, and the Convolutional Neural Network (CNN) (Neyns & Caters, 2022).

Table 2.2.
Overview of the classification approaches used for Urban Green Spaces on high spatial resolution imagery (Neyns & Caters, 2022)

Classification approaches		
Machine learning		Library based classification
Supervised learning		
Parametric	**Non-parametric**	
Minimum distance	K Nearest neighbor	
Discriminant analysis	Support Vector Machine	Spectral Mixture Analysis & Spectral Angle Mapper
Logistic regression	Decision tree classifier (Random Forest)	
Maximum likelihood classifier	Artificial Neural Network (Deep learning)	

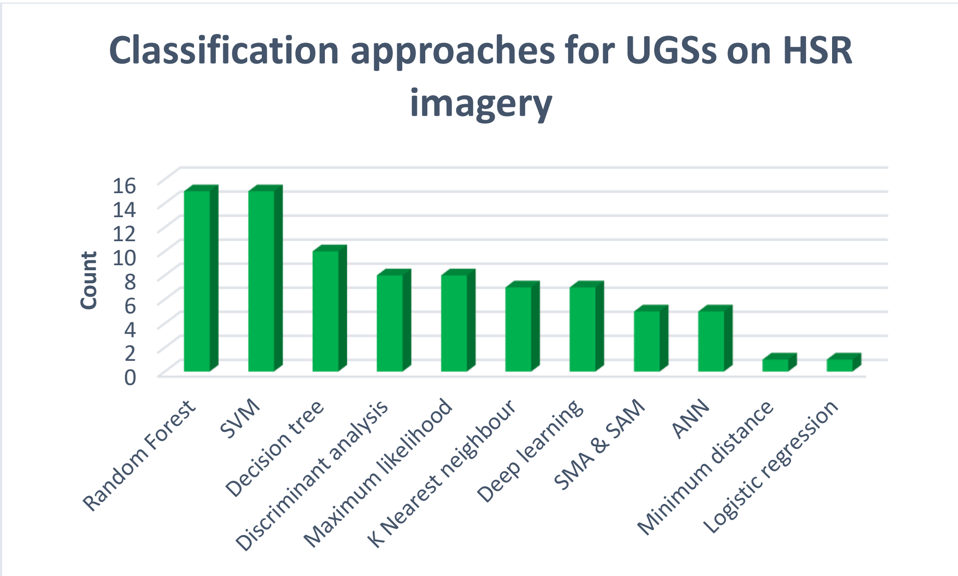

Figure 2.2. Graph depicting the classification approaches for Urban Green Spaces mapping on high spatial resolution imagery and their frequency of appearance in the literature based on the review paper by Neyns and Caters (2022)

The Random Forest (RF) and Support Vector Machines (SVMs) algorithms are the two most popular classifiers in UGSs mapping with HR imagery as shown in Figure 2.2., where either method was used in greater frequency compared with the rest of the methods, in 30 (15 for each method) out of 82 studies. According to a survey comparing the two methods by taking into account a larger set of related papers (251) by Sheykhmousa et al. (2020), SVM and RF are steadily the most used classifiers thanks to their low computational complexity and interpretability capabilities.

RF is a machine learning technique that was first developed by Breiman in 2001, based on an original version introduced by Bell Labs in 1995. It consists of a large number of individual decision trees that operate as an ensemble. More specifically, the RF classifier is comprised of a collection of treelike classifiers which train several classifiers, where each tree contributes a single vote for the assignment thus combining the results through a voting process to find the most popular class **(Fig. 2.3)** (Amini et al., 2018). The integration of multiple classifiers that participate in the ensemble classification decreases the variance and may produce more reliable results. Ensemble methods are divided into boosting and bagging. The latter includes RF and is designed to improve the stability and accuracy of integrated models while reducing variance. At each split, a new sample of predictors is taken, with a user-specified number of predictors (Mtry). RF creates high variance and low bias trees by expanding the random forest to a user-specified number of trees (Ntree). As a result, new sets of input (unlabeled) data are compared to all decision trees formed in the ensemble, and each tree votes for class membership. For the generation of individual decision trees, the best split in the random sample of predictors is picked as the split candidate from the entire set of predictors each time. The membership with the most votes will be the one chosen. The two parameters that need to be defined in a RF model are the number of trees (Ntree) and the number of randomly selected features (Mtry). The Ntree can be as large as possible because the RF classifier is computationally efficient and does not overfit. It is generally accepted that 500 is the best amount for the Ntree, since utilizing Ntrees higher than this number does not increase accuracy. In contrast, the number of Mtry is an optimal value that is determined by the data. In classification tasks, the Mtry parameter should be set to the square root of the number of input features and one-third of the number of input features in regression tasks (Sheykhmousa et al., 2020).

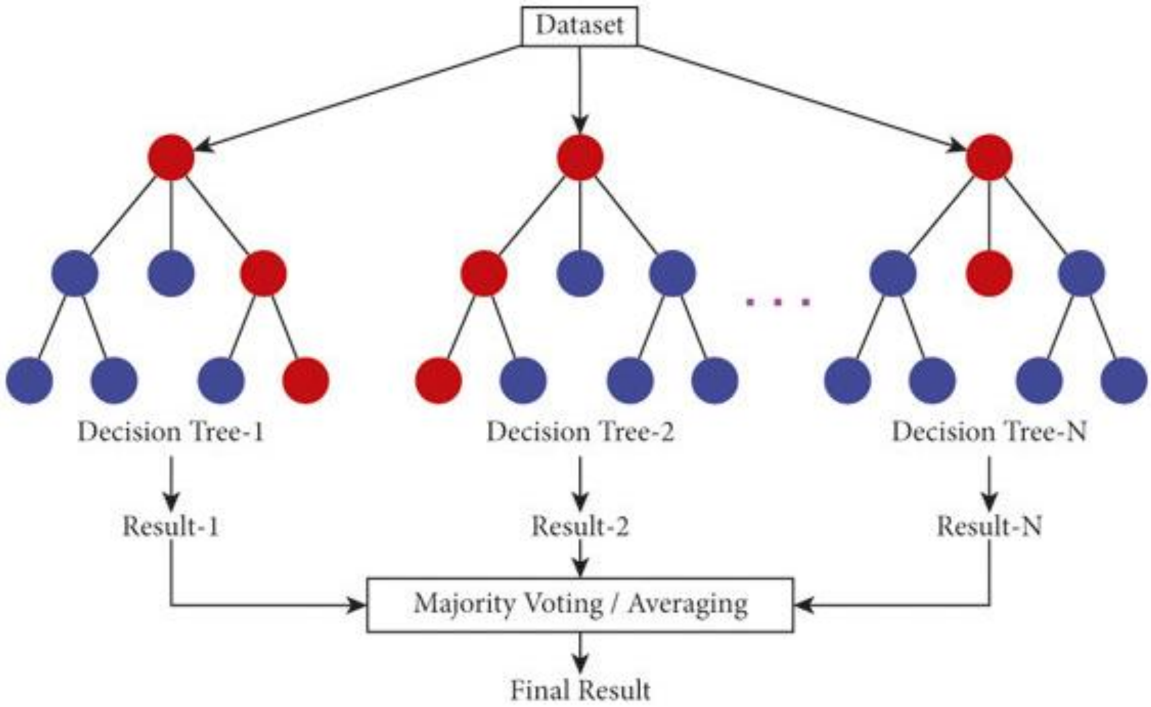

Figure 2.3. Illustration of Random Forest trees (Khan et al., 2021)

RF has been found to be more efficient and stable in land cover related classification studies and provide higher accuracy, in comparison with conventional decision trees (Lebourgeois et al. 2017). The main advantages of RF that have made it the most popular classifier in land cover classification recently are (Sheykhmousa et al., 2020):

a) clear and understandable decision-making process and great results,
b) easy implementation in a parallel structure for data computing acceleration,
c) handling of a large number of input variables,
d) reducing the variance without increasing the bias of the predictions,

e) computing proximities between pairs of cases that can be used in locating outliers,
f) robust to outliers and noise
g) computationally lighter than other tree ensemble methods

The SVM algorithm was first introduced by Vapnik in 1979, based on the principles of statistical learning theory (Dhingra & Kumar, 2019). It is a non-parametric statistical supervised classification method that has been particularly attractive in the field of remote sensing in recent years, due to its ability to successfully handle small training datasets, often producing higher classification accuracy than traditional methods. More specifically, it is a linear binary classifier that assigns a sample to one of two possible classes. The classifier works by determining an optimal hyperplane in order to separate the dataset into a discrete number of predefined classes using the training data, which is what acts as support vectors **(Fig. 2.4)**. Additionally, a portion of the training sample that lies closest in the feature space to the optimal decision boundary is used. These are the most challenging to classify. The learning process that follows selects a number of hyperplanes with no sample between them, and when the margin of separation is maximized, the optimal hyperplane is determined. The selection of the kernel function that generates the dot products in the higher dimensional feature space, highly defines the SVM performance. The most commonly used kernels for remotely sensed image analyses are the polynomial and the radial basis function. Optimizing the SVM parameters may be very resource-intensive. Complications also occur due to the binary nature of the SVMs when used for multi-class scenarios. Since big data classification always tends to be computationally expensive, hybrid SVM methods are used, such as the Granular Support Vector Machine (GSVM) (Sheykhmousa et al., 2020).

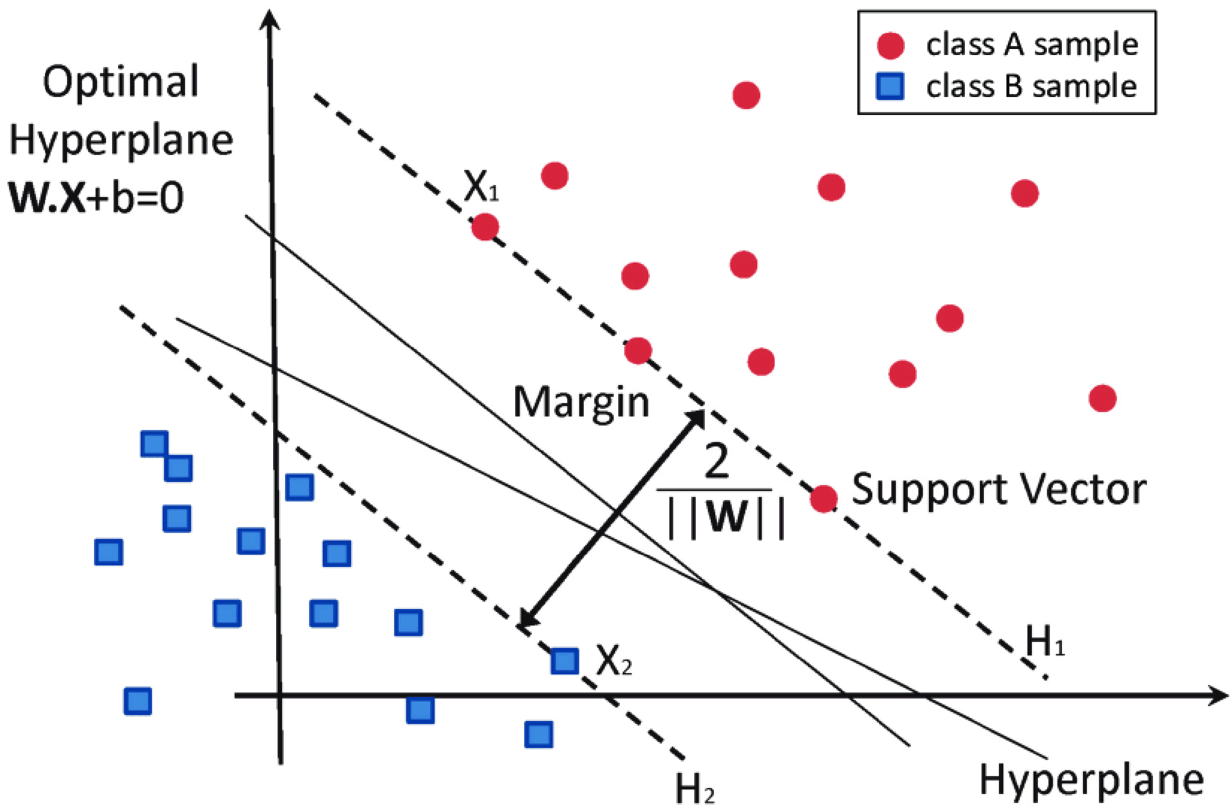

Figure 2.4. Illustration of Support Vector Machines classifier (García-Gonzalo et al., 2016)

SVM is usually preferred on multispectral data, and its major drawback of applicability is the choice of kernel type, as they do not provide an optimal configuration in remote sensing applications (Mountrakis et al., 2011). Its constant use in image classification studies is based primarily on its ability to address the high dimensionality problems and the limited training samples. More specifically, the positive aspects of the classifier are (Sheykhmousa et al., 2020):

a) the use of small training data,
b) one of the most memory-efficient methods,
c) its ability to apply new kernels rather than linear boundaries improving the classification performance.

The main drawbacks of the method are (Sheykhmousa et al., 2020):

a) choosing a suitable kernel,
b) selection of the optimum kernel parameters,
c) relatively complex mathematics behind the classifier, especially for non-experts

2.3. UGSs mapping studies

Huerta et al. (2021) examine the use of 4-band WorldView-2, very high-resolution satellite imagery, and two deep learning techniques to map Urban Green Spaces in the metropolitan area of Monterrey, Mexico. They focus on the semantic segmentation of the specific UGS polygons using convolutional neural network (CNN) encoders on the U-Net architecture. They produce the indices of NDVI, NDWI, and EVI2 to determine their potential for UGS segmentation, which is the result of clipping the image with mosaic fishnet into orthomosaics. Among the produced data, 85% is for training, 14% for validation, and 1% for the evaluation of the method. They implement 24 semantic segmentation models via CNN and afterward they perform its evaluation with metrics of Intersection over Union, Recall, and the computation of a confusion matrix. They suggest that the high accuracy of the results, namely 0.94 for the Kappa coefficient, demonstrates the usefulness of the method in UGS extraction and database updating for urban management.

Chen et al. (2021), in their study on rapid mapping and annual dynamic evaluation of urban spaces on Google Earth Engine (GEE), use Sentinel-2 imagery provided by the Image Collector of GEE to extract and classify the UGS of Beijing, China. Their analysis is based on vegetation indices, textural features, image reduction, and a threshold segmentation in order to differentiate vegetation from non-vegetation. The final classification of the image is performed with the use of three machine learning techniques, namely CART, SVM, and Random Forest, whose results are validated with a confusion matrix. The highest Overall Accuracy is performed by RF at 94%. They go on successfully performing a time series rapid mapping and a dynamic evaluation of the UGS by quality indicators with high accuracy. The authors claim that their workflow shows great potential and it is ideal and cost-effective, especially for cities that experience high urban dynamism.

The purpose of Shekhar & Aryal's (2019) study was to map in ward and grid-level analysis the spatial distribution of the Urban Green Spaces in Kalaburagi, India, using object-based image analysis on very high-resolution imagery. Their analysis begins by pan-sharpening 9 4-Band GeoEye tiles in order to enhance the spatial resolution, then followed by mosaicking them in a single image. The segmentation of the image is performed after many trials that determined the final scale of 30. A fuzzy rule-based classification of the segmented image is realized using eCognition software based on the NDVI and brightness variables, classifying the image into two classes; Green and Non-Green. A second segmentation follows based on the classification results, the chess board segmentation, in order to help in the extraction of the objects of interest. The accuracy assessment is carried out of two error matrices; one using sample statistics and one using Test and Training Area mask statistics. Both revealed the very high Overall Accuracy of the results, with the former getting 95% and the latter reaching 99.8%. They suggest that GEOBIA is ideal for UGS mapping and quantification.

Haas and Ban (2017) investigated the potential use and fusion of one Sentinel-1A C-band SAR and one Sentinel-2A MSI image for a GEOBIA classification and mapping of ecologically important urban and peri-urban space in Zurich, Switzerland, and to introduce spatial characteristics into ecosystem service analyses based on remotely sensed data. For the part of the analysis that the classification of the image is concerned, their work includes the co-registration of the two images and their resampling to 10 m of spatial resolution. They perform the segmentation of the image using the KTH-SEG, an edge-aware region growing and merging algorithm. They use the SVM classifier to classify the segmented image in 12 classes, following CORINE land cover's classification scheme. The accuracy assessment is performed with a minimum selection of 1000 validation pixels, giving out an Overall Accuracy of 79.8% and K_c of 0.78. The authors suggest that the methodology followed on the specific datasets is recommended.

Kopecká et al. (2017) discussed the human well-being provided by the ecosystem services of the urban green spaces and analyze their distribution and extension among three Slovak cities. For the extraction of the urban green spaces, they use Sentinel-2A imagery and a supervised, pixel-based approach to classify the images. They collect a total set of 435 sample plots and use the maximum likelihood classifier to classify the image on a 3-classes-scheme of impervious, water, and vegetation on SNAP and ArcGIS Desktop 10 software. The accuracy assessment of the results is examined via an error matrix table where the Overall Accuracy reaches 90.8% and the Kappa coefficient the value of 0.86. The authors conclude with the usefulness of the method and the S2A imagery and point out that the morphology of the urban fabric may affect the results due to cross-pixel spectral contamination.

Zylshal et al. (2016) investigated the extraction of urban green spaces in Jakarta, Indonesia, with the use of an SVM object-based image analysis approach and Pleiades-1A pan-sharpened and 4-band imagery. They begin by generating the NDVI, NDWI, and MSAVI layers which they use later in the classification. The image is imposed in two segmentations, the second on top of the first, as a means to combine objects with similar characteristics. Support Vector Machine classifier then classifies the image after collecting training samples in 3 classes; vegetation, non-vegetation, and water. The parameters of texture, brightness, and contextual information are then used for a Rule-Based Refinement of the SVM classification to improve results. An Area-Based accuracy assessment is conducted by using 20 randomly selected point samples in a 100 m radius, giving out a high Overall Accuracy of 86%, while at the same time, 92% of the areas classified as vegetated are correct. The authors suggest that this method is suitable and more efficient for urban green space monitoring in comparison with pixel-based classification techniques but also point out the weakness of the EO data in relation to the different sensors and data acquisition time.

Feng et al. (2015) looked into the use of ultra-high resolution Unmanned Aerial Vehicle retrieved images to map urban vegetation with a hybrid method of texture analysis and the Random Forest classifier. Three different vegetation types are distinguished as separate classes for the classification according to their texture which is derived from the gray-level co-occurrence matrix (GLCM), along with the classes of bare soil, water, and impervious surfaces. The Random Forest classification technique involves two random selection steps; a bootstrap strategy where about 2/3 of the training samples are randomly selected with replacement to build each decision tree, and an inner cross-validation to evaluate the classification accuracy of Random Forest which includes the remaining 1/3 samples, known as out-of-bag (OOB) data. The classification is performed in the form of a confusion matrix with training samples that sum a total of 500 pixels for each class. The authors suggest that the high overall accuracy that ranges between 90.6% and 86.2% of the two areas tested demonstrates the outstanding capabilities of the UAVs, however, they point out the importance of the inclusion of a NIR band alongside the RGB bands in the analysis for better data acquisition.

2.4. UGSs operational products

This section aims to provide a review of the current open-access operational products available for LU/LC and therefore UGSs. Thus far, the existence of such datasets is limited to municipality-level coverage or pan-continental and national platforms. In any of these cases, the quality is usually insufficient for analyses on UGSs (Ludwig et al., 2021). In the case of Greece, such products are available only for national parks and other wildlife-protected areas, but not for UGSs.

2.4.1. Urban Atlas

The Urban Atlas (UA) has been used by several papers in regard to the study of UGSs (Madureira & Andersen, 2013; Wüstemann et al., 2017; Feltynowski et al., 2018; Kolcsár et al., 2021). The UA 2018 is a very high-resolution land use and land cover dataset provided by the European Union's Copernicus program, with the support of the European Space Agency and the European Environment Agency (European Commission, 2020). It offers LULC for 788 Functional Urban Areas with a population of over 50,000 inhabitants of the EU, EFTA, the West Balkan countries, the UK, and Turkey. It also contains population estimates and Street Tree Layers (STL). The cartography is based on the classification and interpretation of 2 to 4-meter-resolution satellite imagery provided by satellite systems like Pléiades, KOMPSAT, Planet, SPOT6, and SuperView (European Commission, 2020). The LULC of the UA is divided into 5 main classes, which in turn are divided into further subclasses. Class 1 includes artificial surfaces, Class 2 agricultural areas, Class 3 natural and semi-natural areas, Class 4 wetlands and Class 5 water (Kolcsár et al., 2021). Though the minimum mapping unit of Class 1 is 0.25 ha and for Classes 2 – 5 is 1 ha, there are cases where polygons of smaller size can be found near the edges of the FUAs or when bordering the sea (European Commission, 2020). The overall accuracy of the final product is 87.5%, while the artificial surfaces of Class 1 have 93.61% and the rural areas of Classes 2-5 resulted in OA of 86.45% (Copernicus, 2021).

2.4.2. Open Street Map

OpenStreetMap (OSM), founded by Steve Coast in 2004, is a free, digital, and editable worldwide map that is being built by volunteers largely from scratch and released with the open-content license of Open Data Commons Open Database License (ODbL) (OSM, 2022). The data that relate to green spaces are limited to public ones only, as the private ones are usually excluded from mapping in OSM (Ludwig et al., 2021). At the same time, there is inconsistency in the way green spaces are mapped and some areas remain incomplete. The process followed by the users to create objects, as is the case with UGSs, is basically the digitization of public domain high-resolution satellite or aerial imagery, such as Bing, Digital Globe Imagery, and Esri World Imagery. In contrast with other tags, vegetation and urban vegetation-related ones are categorized in a variety of forms. Therefore, the representation of UGSs in different regions is complicated and makes it impossible for them to be universally defined as one set of tags, which is something that should be taken into serious consideration when using the data (Ludwig et al., 2021). As a result, there are few authors that use OSM data for UGSs-related studies, though their use in geosciences applications has been widespread, mostly for improving its quality and training models for navigation and land use classification (Vargas-Munoz et al., 2021).

2.5. Final remarks

This chapter covered the available literature on UGSs mapping and the methods and techniques used for this purpose. The main findings of the chapter are as follows: i) There is an increased necessity for the preservation and expansion of UGSs, also stressed by international organizations, as their significance for the quality of life in cities is crucial. ii) High-resolution imagery is preferred in the literature more recently and it is ideal, especially when it can be retrieved free of charge, which is important for the cost-effectiveness of the studies. It also gives away better results in binary classifications for the simple extraction of green spaces, as the spectral resolution is not essential like in cases where different vegetation species need to be classified. iii) The most appropriate and preferred analysis technique in literature is the OBIA, either by itself or used in a combination with other techniques, as the increase in its use and study has been steadily overcoming the obstacles posed by the complications of the segmentation process. iv) RF and SVM are the most widely used non-parametric classifiers in UGSs classification. v) There is a lack of operational products that cover the clear distribution of UGSs as opposed to their land use at a national and international level, creating the need for their creation.

These findings were the driving factor for the selection of the methods, data, and study area that this thesis is set to investigate, as discussed in the proceeding chapters.

Chapter 3: Study area and datasets

3.1. Study area

Athens is Greece's capital and largest city, located in the southeast of the Greek mainland with a population of around 3.8 million inhabitants. The Greater Athens Area covers a surface of around 360 km^2. Athens enjoys a typical Mediterranean climate (Csa in Köppen's climate classification), with hot, dry summers and mild, rainy winters. The mean annual temperature of central Athens for the period of 1955-2010 is 17.8^{o}C, with an amplitude of 19.5^{o}C (minimum monthly average 8.8oC in January, maximum monthly average 28.3^{o}C in July). The average amount of precipitation for the same period is 411.8 mm, though the value may vary by up to 100 mm depending on location (HNMS, 2022). The city lies within the basin of Attica surrounded by mountains on all sides except for the south, where it is bounded by the Saronic Gulf in the Aegean Sea. Due to its topography and several other factors, such as the urban sprawl and the destruction of the peri-urban forests by wildfires, the city experiences intense air pollution and the Urban Heat Island effect which has an intensity of as high as 10^{o}C (Gaitani et al., 2011). Athens started to experience spontaneous, undesigned urban development in areas with undefined land uses starting in the 1920s onwards, with the uncontrolled and unplanned outward expansion of the urban web continuing to this day (Chorianopoulos et al., 2010; Kassomenos et al., 2022). This resulted in a lack of open public spaces and a low quality of environmental infrastructure (Chorianopoulos et al., 2010). Green spaces in Greece are regulated by law 4280/2014, article 27, in the same framework as other common areas that include sidewalks, pure sidewalks, bike paths, squares, groves, greenery, and playgrounds, as well as free spaces of urban and suburban green (GMEE, 2014). Therefore, the green areas in the city are few in number and rather small in size. The majority of them are scattered within the city, found mostly on the hills in the basin or on the mountains surrounding it. As a result, only just 0.96 m^2 of green space corresponds to each inhabitant in Athens, when the World Health Organization places 9 m^2/person as the minimum figure (WWF, 2020).

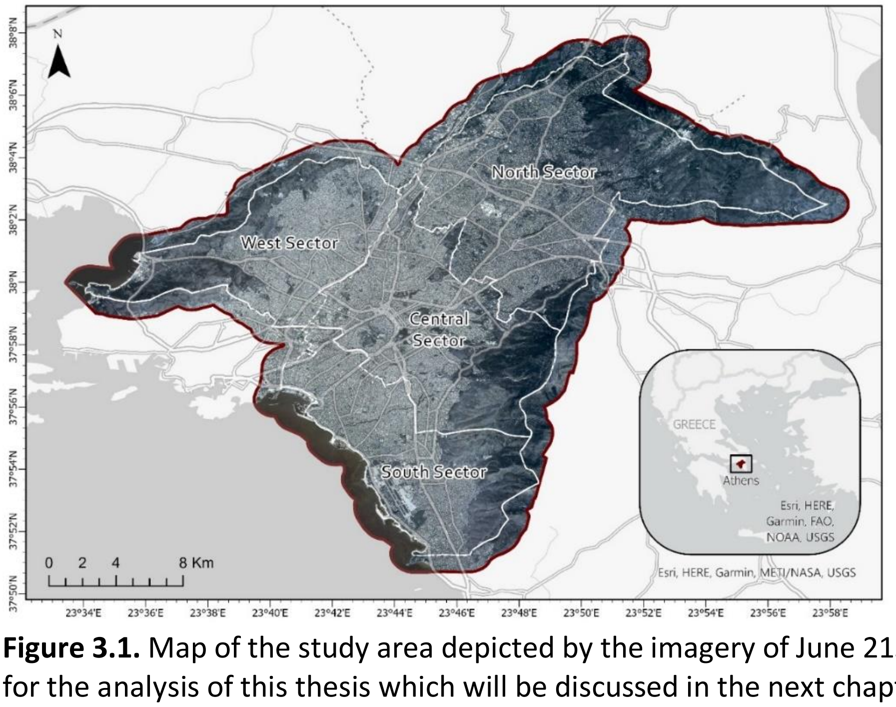

Figure 3.1. Map of the study area depicted by the imagery of June 21st, 2020 obtained by Planet for the analysis of this thesis which will be discussed in the next chapter, with a 1km buffer zone of the Greater Athens' limits

3.2. PlanetScope imagery

PlanetScope imagery is one of the two imageries used in this thesis for the implementation of the methodology for the extraction of the Urban Green Spaces in Athens. PlanetScope is a constellation of about 130 Dove satellites operated by Planet, capable of imaging the whole land surface of the Earth daily, with a collecting capacity of 200 million km^2/day and image resolution of 3 meters per pixel (Planet, 2021). The satellites carry three types of instruments for the capturing of the images. The PS2 and PS2.SD telescope instruments generate 4-band images (see **Table 4.1.**) while their main difference is found in their passband filters, as the PS2.SD is interoperable with those of Sentinel-2. The PSB.SD instrument has a larger sensor, adding the Red Edge as its fifth band (Planet, 2022).

Table 3.1.
PlanetScope PS2 instrument's spectral information

PlanetScope PS2		
Bands	Spectral Region	Wavelength (nm)
Band 1	Blue	464 - 517 nm
Band 2	Green	547 - 585 nm
Band 3	Red	650 - 682 nm
Band 4	NIR	846 - 888 nm

More specifically, 20 cloud-free, analytic surface reflectance, multi-spectral PS2 scenes, for a single date, were downloaded from Planet Explorer (**Fig. 3.1.**). The scenes were captured by four different satellites on June 21st, 2020, between 08:22:47 am and 08:55:46 am (see **Table 3.2.**)

Table 3.2.
PlanetScope dataset used for the extraction of the green urban areas in Athens

Satellite	Product	Satellite ID	Number of images	Acquisition time	Acquisition date	Bands	Resolution (m)
PlanetScope	OrthoScene (SR)	2257	3	08:22:47 - 08:22:52	21/06/2020	B, G, R, NIR	~3
		0f4e	7	08:52:57 - 08:53:03			
		100a	7	08:53:07 - 08:53:14			
		106d	3	08:55:42 - 08:55:46			

3.3. Sentinel-2 imagery

The European Copernicus program was set up at the initiative of the European Commission in cooperation with the European Space Agency as a follow-up to the GMES (Global Monitoring for Environment and Security) program for global monitoring of the environment and security. Its primary objective is the study and monitoring of the Earth's surface environment. It covers a wide range of applications relating to climate change, emergency management, security, etc. (Perakis, 2015). It is a set consisting of different types of data collection systems and instruments drawn from various sources. More specifically, it consists of Earth surface observation satellites, airborne platforms equipped with specific sensors and recorders of the Earth's surface, and finally fixed sensors to collect and record the various parameters and variables related to the Earth's environment (ESA, 2022).

For the operational needs of the Copernicus program, the European Space Agency (ESA) has developed a family of satellites called Sentinel. The Sentinel-1 satellite is an active all-weather satellite system and it is used for surveys on the Earth's land surface and in the oceans. Sentinel-2 is a passive satellite system that includes multi-spectral imaging (MSI) instruments, used for environmental monitoring, water studies, and ground coverage. Sentinel 3 satellite has several instruments and can measure surface temperature, sea level differences, and ocean color with high accuracy. Sentinel 4, 5 and 6 Precursor satellites are designed for atmospheric analysis. Sentinel 6 has a radar that allows recording altitude differences in the oceans and studying climate change with high accuracy (Perakis, 2015).

Sentinel-2 is a twin satellite system (Sentinel-2A and Sentinel-2B) with a wide swath width recording instrument at 290 km and a multi-spectral imager covering 13 spectral bands (443 - 2190nm) showing three spatial resolutions of 10, 20, and 60 meters. Sentinel-2A was launched on 23 June 2015 and Sentinel-2B on 7 March 2017. They operate simultaneously, phased at 180° to each other, in a sun-synchronous orbit at a mean altitude of 786 km (ESA, 2022) and a revisit cycle of 5 days (ESA, 2022; Parcharidis, 2015). The Sentinel-2 products are available in two types; Level-1C (LC1) contains the image with Top-Of-Atmosphere reflectances and Level-2A (LA2) with Bottom-Of-Atmosphere reflectances. Their expected mission duration is 7 years (Perakis, 2015).

In this thesis, one L2A image of the Sentinel-2A MSI satellite will be used. The image ought to be at around the same time as the one retrieved from PlanetScope. The closest cloud-free image that was available was on June 29th, 2020, and was retrieved from Copernicus Open Access Hub. For the analysis, only the Blue, Green, Red, and Near-Infrared (NIR) were used, as shown in bold in **Table 3.3.**

Table 3.3.
Sentinel-2A spectral information. The bands in bold are the ones used for the analysis

		Sentinel-2A MSI	
Band	Spectral Region	Central wavelengths (nm)	Spatial Resolution (m)
Band 1	Coastal Aerosol	442.2	60
Band 2	**Blue**	**492.4**	
Band 3	**Green**	**559.8**	**10**
Band 4	**Red**	**664.6**	
Band 5	Vegetation red edge	704.1	
Band 6	Vegetation red edge	740.5	20
Band 7	Vegetation red edge	782.8	
Band 8	**NIR**	**832.8**	**10**
Band 8A	Narrow NIR	864.7	20
Band 9	Water vapor	945.1	60
Band 10	SWIR - Cirrus	1373.5	
Band 11	SWIR	1613.7	20
Band 12	SWIR	2202.4	

3.4. Urban Atlas data

For this study, the FUA of Athens which covers the whole region of Attica, as seen in **Figure 3.2.**, was downloaded from the website of Copernicus, in order to extract the polygons of the class of Green Urban Areas (GUA), as a means of validation of the classification results. The accuracy of the specific FUA is not provided by the Urban Atlas 2018 Validation Report. However, the validation of the product in the regions of Greece and Cyprus shows an OA of 92.63% for urban classes, which include the GUA (Copernicus, 2021).

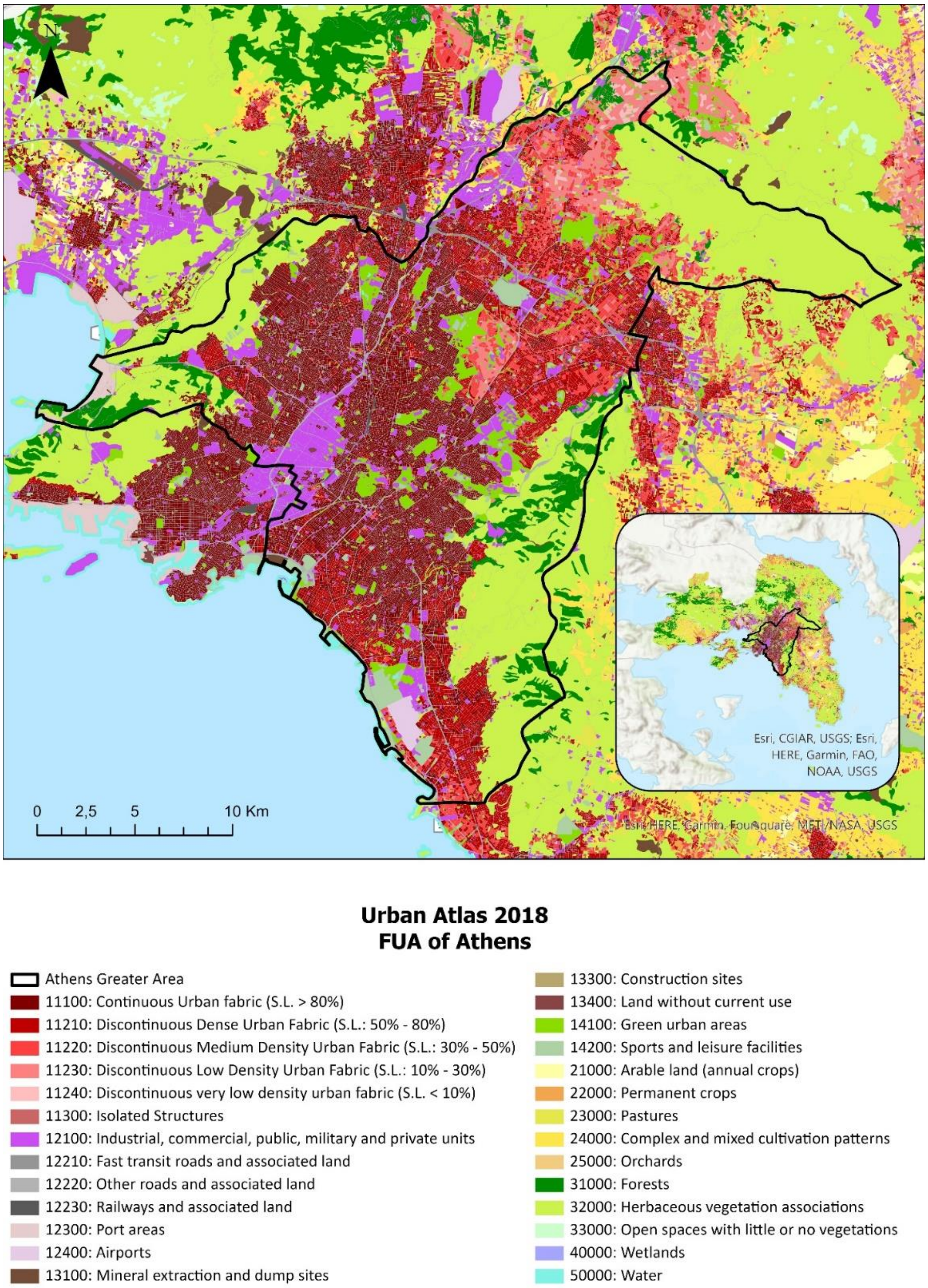

Figure 3.2. Map depicting the Urban Atlas' 2018 Functional Urban Area of Athens and the boundaries of the Greater Athens Area

Chapter 4: Methods

The Geographic Object-Based Image Analysis (GEOBIA) methodology used in this thesis to extract the Urban Green Spaces includes the segmentation and classification of the PlanetScope satellite imagery by generating training samples and accuracy assessment points, training the algorithm with the Random Forest (named Random Trees on ArcGIS, therefore, mentioned as such here forth) and SVM classification techniques, finally generating the accuracy assessment statistics. The sequence of steps followed to perform the methodology and produce the final urban green spaces maps is summarized in a flowchart in **Figure 4.1.**

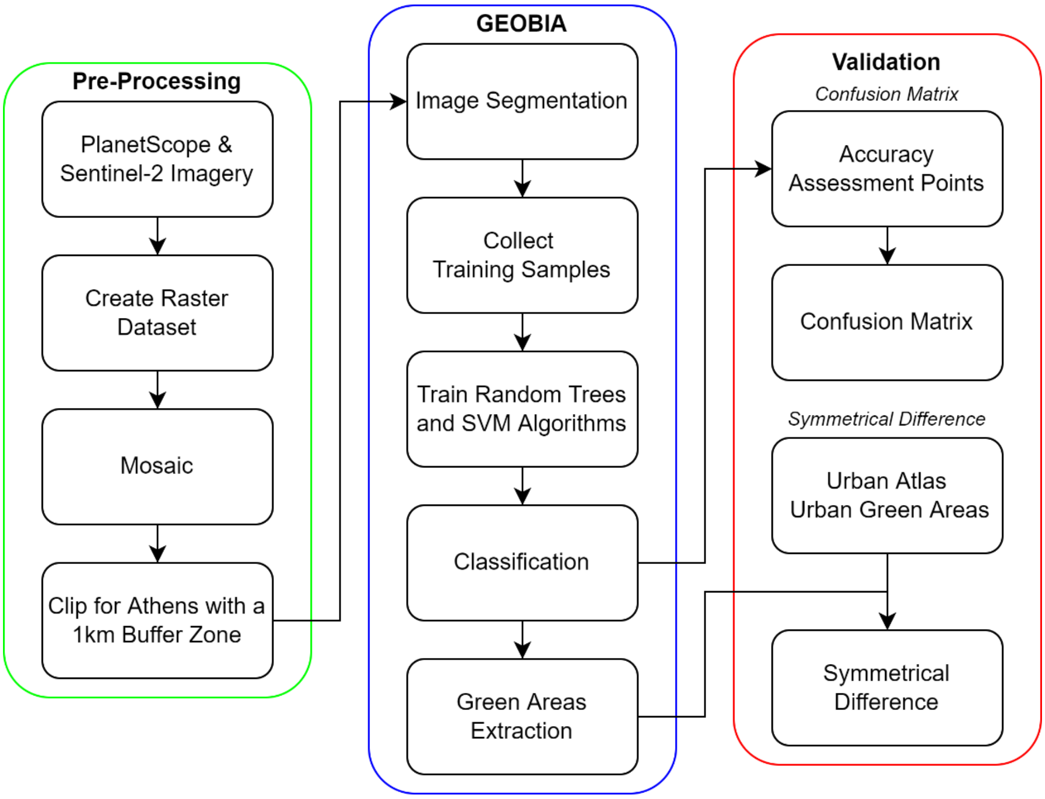

Figure 4.1. Flowchart of the methodology followed for the extraction of the green areas

4.1. Data Pre-processing

The PlanetScope scenes were clipped directly from the website using a region of interest covering the area of Greater Athens and were downloaded already atmospherically and geometrically corrected, therefore no additional preprocessing was required. Since the scenes were 20, some of which overlapping each other, they were merged into a single raster dataset. As the Sentinel-2 product type used is L2A, no additional atmospherical correction was needed either. The 4 bands needed for the analysis were merged in one single multiband raster layer with the Composite Bands function.

Finally, for analysis purposes, both raster datasets were clipped with a buffer zone of 1 km around the limits of the Greater Athens Area, obtained by the Greek open geodata catalog, in order for water surfaces to be included in the classification and to avoid spectral confusion.

4.2. GEOBIA description

GEographic Object-Based Analysis (GEOBIA) is a discipline of Geoinformatics that relies on remote sensing imagery and involves the segmentation of its pixels into image objects, that are spatially, spectrally, and texturally homogenous (Hay & Castilla, 2008). This approach reduces the accuracy problems usually found in pixel-based analyses of VHR imagery and improves the performance of image classification which is what has brought its gradual prominence in the past couple of decades (Souza-Filho et al., 2018; Simionato et al., 2021).

The segmentation of the Athens images was conducted by the segment mean shift tool using the false-color composite with bands 4, 1, and 2 for the PlanetScope image and bands 8, 4, 3 for the Sentinel-2 image (NIR, RED, GREEN), in order to create a clearer representation of vegetation. The scale parameter selection is still subjective and user-dependent and it can directly affect the accuracy and efficiency of the segmentation (Ming et al., 2015). In this case, after various experimentations with the parameters, spatial and spectral details were given the highest value available of 20, while the minimum segment size was set at 5 pixels. This selection proved to perform a better representation of the land cover since the dense urban landscape requires high detail to distinguish the studied features (ESRI, 2022a).

For the training of the algorithm, training samples were collected from within the segmented images using the Training Samples Manager. It was decided the images to be classified into 3 classes to avoid confusion since the objective was only the extraction of the green spaces. Therefore, two sets of 200 samples were collected for each of the three following classes; Green Areas, for vegetation, Developed Areas for impermeable surfaces, such as buildings, streets, rocky and bare soil, and Water for the sea, lakes, rivers, and swimming pools. The selection of the training samples was performed by drawing polygons within the segmented objects based on the visual interpretation of the segmented false-color images and their spectral separability **(Fig. 4.2)**.

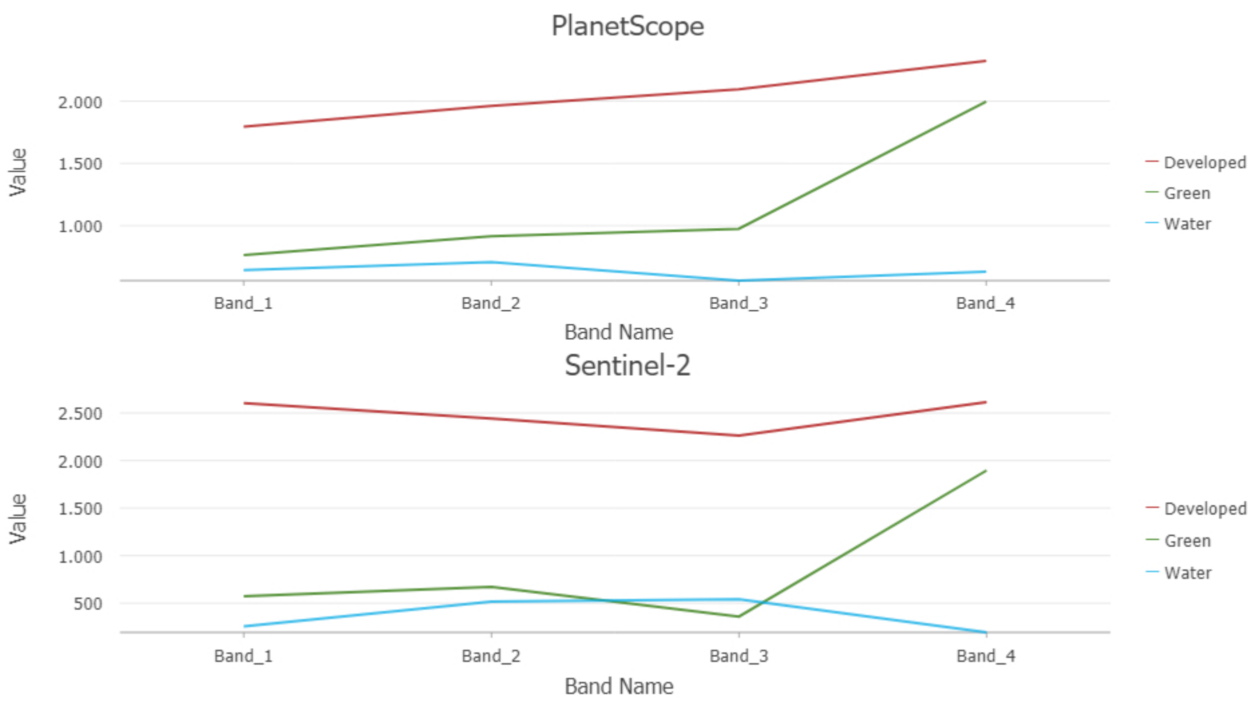

Figure 4.2. Spectral profiles of the training samples collected for the three classes in the PlanetScope (up) and Sentinel-2 (down)

The algorithm was trained with the classification methods of Random Trees and Support Vector Machine, two machine learning algorithms. The Random Trees classifier consists of a collection of individual decision trees in which each tree is generated from different samples and subsets of the training data (ESRI, 2022b). The SVM classifier is a particular linear classifier that is based on the margin maximization principle. It performs structural risk minimization, which improves the complexity of the classifier with the aim of achieving excellent generalization performance (Adankon & Cheriet, 2009). Neither of the classifier tools provides any sort of user parametrization options, as the software provides the algorithms on default. The trained files were used to classify the images which were then converted to vector format and the green areas were extracted to separate layers.

The four final layers of green spaces were finally imposed on dual comparisons regarding the land they cover with the Symmetrical Difference tool for statistical reasons. This tool computes a geometric intersection of the input and update features, returning the input features and update features that do not overlap. The comparisons were performed as follows: Random Trees vs SVM for the PlanetScope and Sentinel-2 images respectively, as well as PlanetScope vs Sentinel-2 images on the SVM and Random Trees classifiers.

4.3. Validation approach

The validation was performed by generating accuracy assessment points with random stratified sampling, where the population gets divided into homogenous groups called strata, from which random samples are then drawn in a number proportional to each stratum's size compared to the total population (Glasgow, 2005). For a better and more objective understanding of the results, four different sets of accuracy points were generated; 25, 50, 100, 250, 400, and 500 points. In each case, a different number of samples was taken for each of the three classes according to the percentage of the land they cover in the study area. For the 500 points, the class of Water was assigned 24 sample points, the Green Areas 213 and the Developed Areas 263. The initial PlanetScope or Sentinel-2 images, depending on the case, and ESRI's World Imagery basemap were then used as reference data to assess the accuracy of the classified maps and fill in the ground truth fields on the layers' attribute tables. The confusion matrix – a table presenting the summary of prediction results on a classification – for every set of points was then created by using the accuracy assessment points layer as input.

The Urban Atlas 2018 for Athens was also used as reference data to compare the results of the classified urban green spaces with the UA's class of Green Urban Areas, which includes public green areas for predominantly recreational use such as gardens, playgrounds, zoos, parks, castle parks and cemeteries (European Commission, 2016). For the comparison to be made, the GUA class was extracted from the UA layer and was used to clip the classified green areas to exclude the suburban forested areas and other large or very small green areas. The symmetrical difference tool was used to calculate the difference between the land covered by the paired layers.

Chapter 5: Results

The methodology performed on one PlanetScope and one Sentinel-2 image using two different algorithms resulted in 4 classification maps **(Fig. 5.1.; Fig. 5.2.)**. All four maps show a similar pattern of the distribution of the three classes across the study area. The geographic and anthropogenic features of the city are easily distinguishable. The results of the classification reveal the extension and high density of the artificial surfaces in the city. Developed or impermeable surfaces cover most of the central part of the study area where the city of Athens is spread across. Among them, some of the features that can be recognized are streets and highways, airports, seaports, and even quarries. The green surfaces are distributed mostly on the fringes of the city limits on three sides; West, Northeast, and East. These vegetated areas are actually mountains that surround the plain area where the city lies, forming a basin. If those mountains were to be excluded, it is quite obvious that the green areas in Athens are rather scarce. In the interior of the urban fabric, the green spaces are concentrated mostly in hilly areas, along the streets, or in some of the few streams and rivers that remain uncovered by concrete. It is also quite apparent that the northern suburbs have a much higher green ratio than the rest of the city, as they are built within forested areas on the slopes of mounts Penteli and Hymettus. Finally, the water class is mostly found on a few artificial lakes and swimming pools across the city.

The results of the classifications and the differences between each algorithm and satellite imagery are presented in more detail in this chapter.

5.1. PlanetScope imagery

The results of the Random Trees classifier are shown in **Fig. 5.1.** and the coverage statistics are in **Table 5.1.** As already mentioned, the extension and high density of the artificial surfaces are apparent. Developed or impervious surfaces cover an area of 212.36 km^2 or 59.02% of the total area. They are found all across the basin formed by the mountains, as well as on rocky or bare soil patches of land in the mountainous areas. Water surfaces cover only 1.31% of the study area and they are found mostly in a few artificial lakes, fountains, and swimming pools. The green areas make up 40.62% of the study area and they are concentrated on the western, eastern, and northeastern mountainous fringes of the city limits. The lower part of **Fig. 5.1.** shows a clearer representation of the green areas, by displaying the Green class only.

The SVM classification results are shown in **Fig. 5.2.** and the coverage statistics are in **Table 5.1**. Here, in contrast with Random Trees, the green areas take up a larger percentage of the area's surface, at 46.12% or 165.95 km^2. The lower part of **Fig. 5.2.** shows a clearer representation of the green areas, by displaying the Green class only. The developed/ impervious surfaces come in first in surface coverage, at 53.73% or 193.31 km^2. Finally, the water class covers only just 0.55% or 0.15 km^2 of the study area.

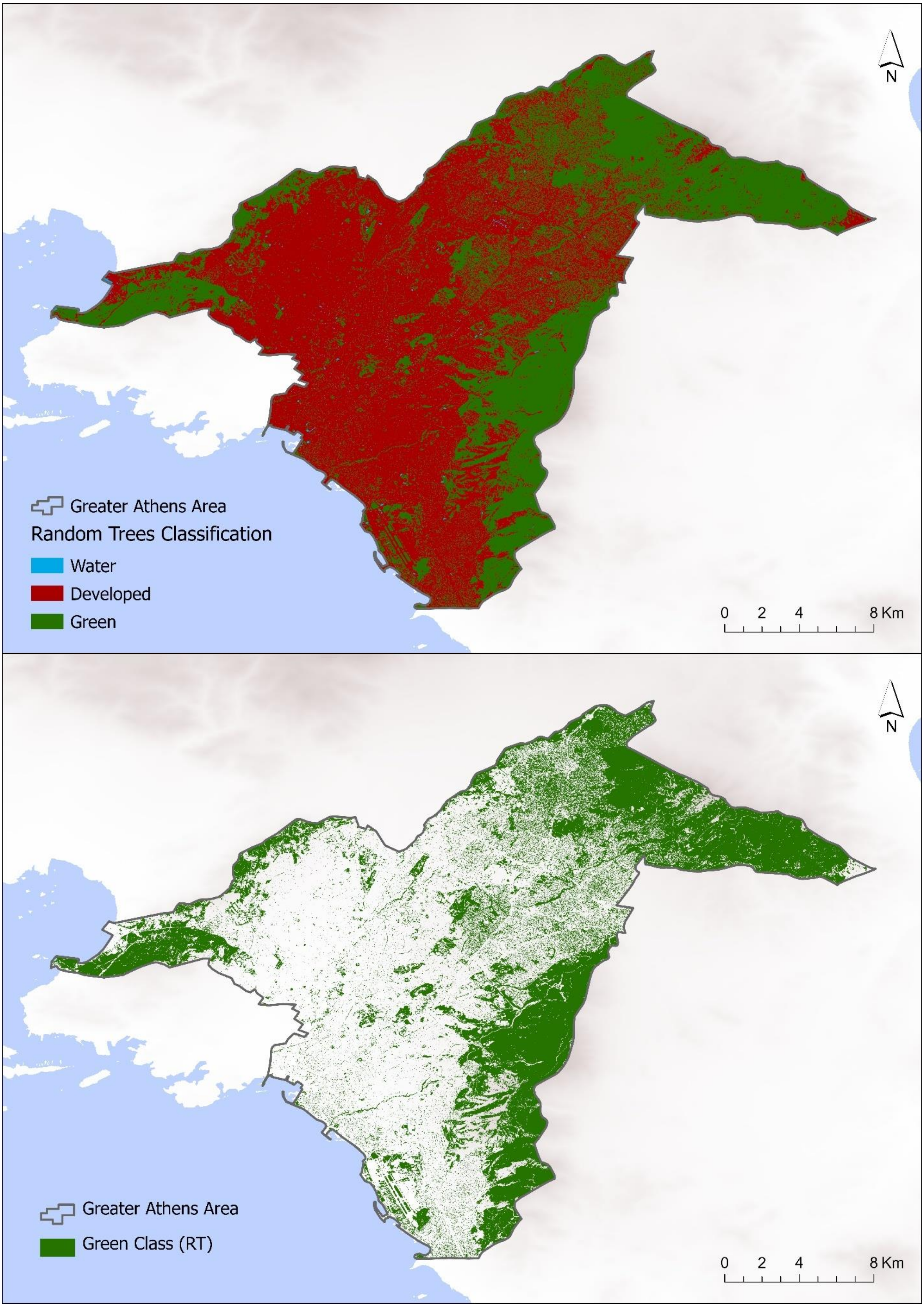

Figure 5.1. Classification results (above) and extracted green areas (below) of the Greater Athens Area using the GEOBIA method and the Random Trees classifier on the PlanetScope imagery

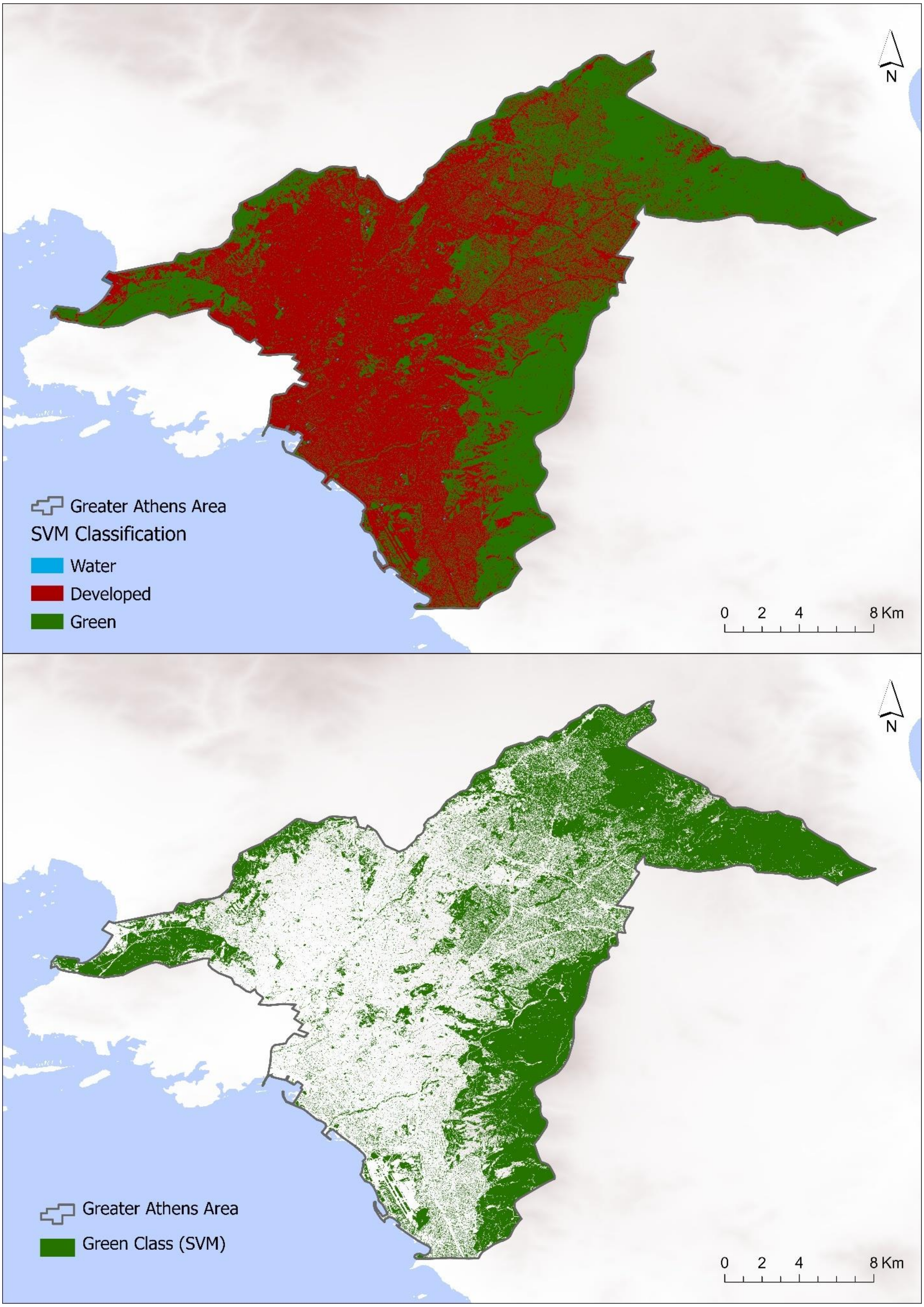

Figure 5.2. Classification results (above) and extracted green areas (below) of the Greater Athens Area using the GEOBIA method and the SVM classifier on the PlanetScope imagery

Table 5.1.
Surface coverage statistics of the RT and SVM classifiers for the PlanetScope imagery

	Random Trees		SVM	
Class	**Area (km^2)**	**Percentage (%)**	**Area (km^2)**	**Percentage (%)**
Developed	212.36	59.02	193.31	53.73
Green	146.14	40.62	165.95	46.12
Water	1.31	0.36	0.55	0.15

5.2. Sentinel-2A imagery

The results of the RT classifier for the Sentinel-2 imagery are shown in **Figure 5.3.** and the coverage statistics are shown in **Table 5.2.** The Developed areas take up the largest percentage of the area's surface, at 66.99% or 241.06 km^2. The Green surfaces come in second, at 32.77% or 165.15 km^2. The lower part of **Figure 5.3.** shows a clearer representation of the green areas, by displaying the Green class only. Finally, the water class covers only just 0.84% or 0.23 km^2 of the study area.

The SVM Classifier results are presented in **Figure 5.4.** and in **Table 5.2**. The results reveal, once again, the superiority of the Developed class in terms of coverage, as it takes up the largest percentage of the study area's surface, at 62.71% or 225.63 km^2. The Green surfaces come in second, at 37.06% or 133.33 km^2. The lower part of **Figure 5.4.** shows a clearer representation of the green areas, by displaying the Green class only. Noticeably, the water class covers only just 0.24% or 0.85 km^2 of the study area.

Table 5.2.
Surface coverage statistics of the Random Trees and SVM classifiers for the Sentinel-2 imagery

	Random Trees		SVM	
Class	**Area (km^2)**	**Percentage (%)**	**Area (km^2)**	**Percentage (%)**
Developed	241.06	66.99	225.63	62.71
Green	117.92	32.77	133.33	37.06
Water	0.84	0.23	0.85	0.24

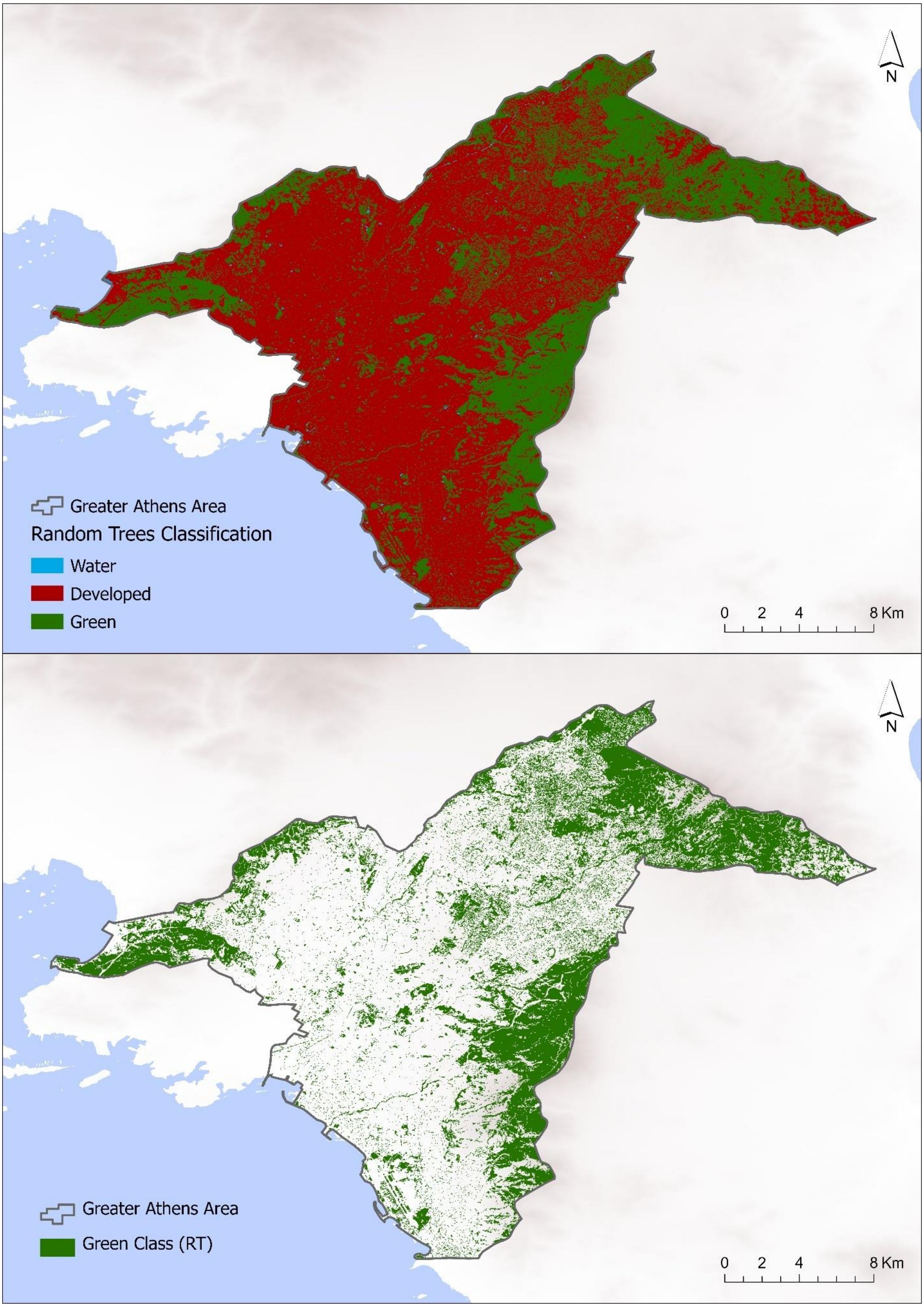

Figure 5.3. Classification results (above) and extracted green areas (below) of the Greater Athens Area using the GEOBIA method and the Random Trees classifier on the Sentinel-2 imagery

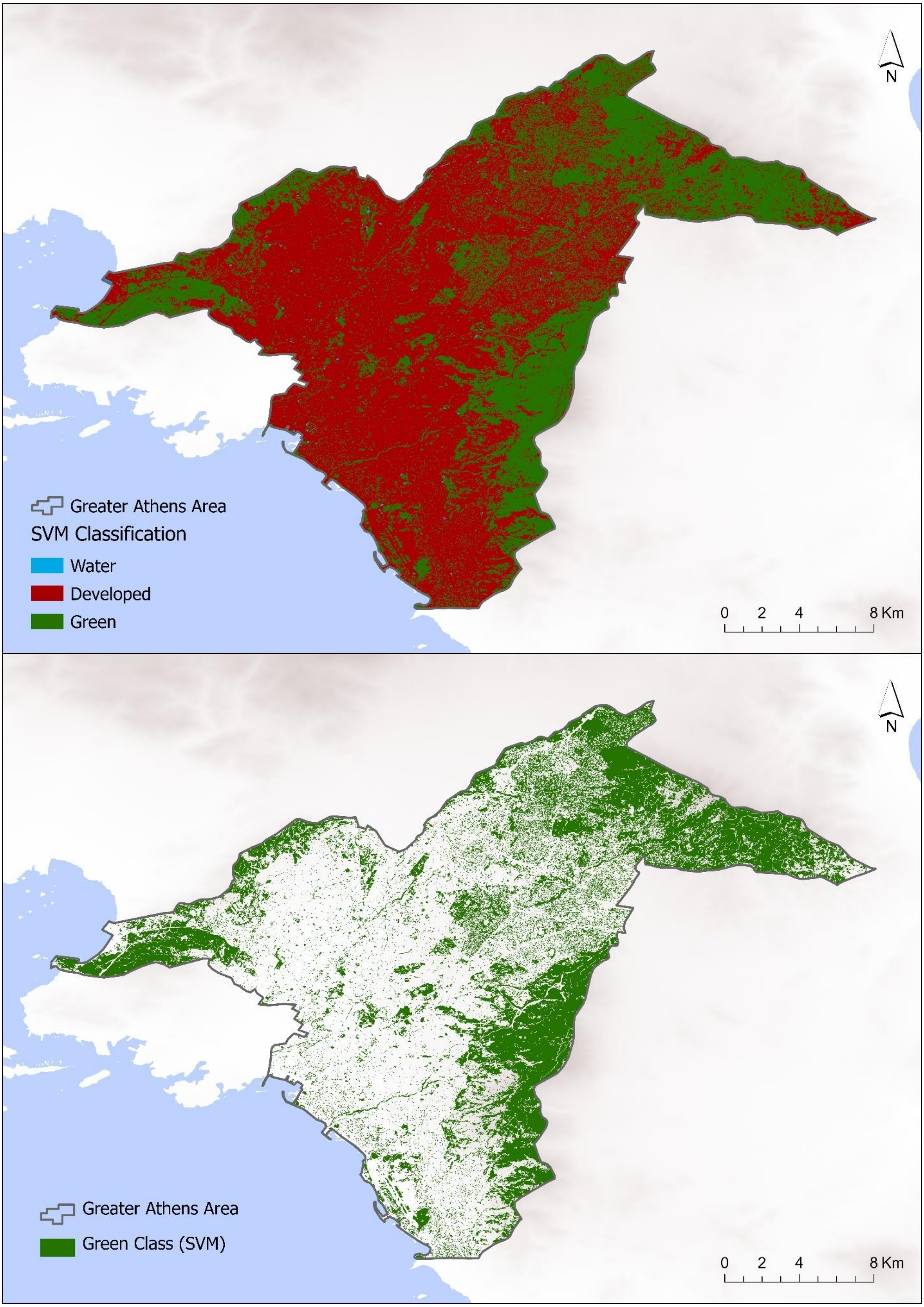

Figure 5.4. Classification results (above) and extracted green areas (below) of the Greater Athens Area using the GEOBIA method and the SVM classifier on the Sentinel-2 imagery

5.3. Comparative analysis

The goal of this section is to illustrate and discuss the difference in the land cover of the green areas that each classifier resulted in, by performing dual comparisons with the Symmetrical Difference tool. Dual comparisons are made between Random Trees and SVM for the PlanetScope and the Sentinel-2 imagery respectively, as well as for the results of the Random Trees classifier between PlanetScope and Sentinel-2 and for the results of the SVM classifier between the two images. For obtaining a more detailed view of the comparison results, each map includes two close-up areas of two regions of the study area in the heart of the basin of Athens.

5.3.1. Random Trees vs SVM with PlanetScope imagery

The Symmetrical Difference performed between the Random Trees and SVM classifiers on the PlanetScope image is presented in **Fig. 5.5.** As seen in **Table 5.3.**, the common area that was classified as green by both classifiers is 143.1 km^2. The RT classified as green 3.04 km^2 of the land surface that wasn't classified as such by SVM. On the other hand, the SVM classified 22.85 km^2 more green areas than the RT. That noticeable difference can be seen in the mountainous areas surrounding the city, with an emphasis on the eastern side of Mt. Penteli, in the far east of the study area. In the urban fabric, the differences are much milder, yet in terms of small green urban areas, this could have a negative impact on their study.

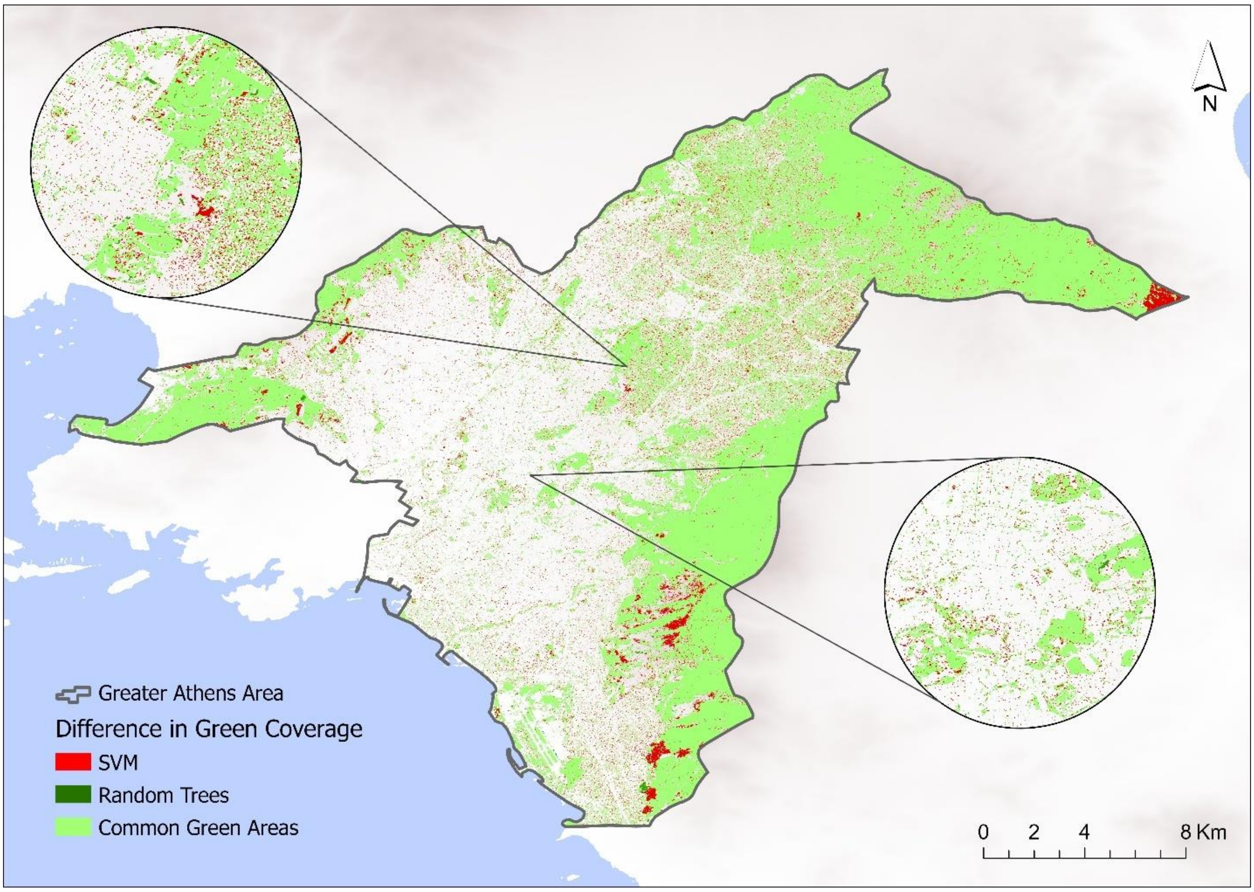

Figure 5.5. Symmetrical difference between the Random Trees and SVM classifiers on the PlanetScope imagery

Table 5.3.
Area comparison between Random Trees and SVM classifiers used on the PlanetScope imagery

Random Trees vs SVM (PlanetScope)		
Extra in SVM	**Extra in RT**	**Common area**
22.85 km^2	3.04 km^2	143.1 km^2

5.3.2. Random Trees vs SVM with Sentinel-2 imagery

The Symmetrical Difference performed between the Random Trees and SVM classifiers on the Sentinel-2 image is presented in **Fig. 5.6.** In this case, the differences seem to be more equally distributed along the study area, yet the mountains appear to have the majority of them. A large concentration of differences can be observed in the northeastern portion of the basin, where there is a greater ratio of green in comparison to the rest of the city. The common green area of the two classifiers is 115.21 km^2, and yet again, the SVM classifier resulted in more land surface classified as green by 18.1 km^2, in contrast with the RT which has classified only 2.71 km^2 of extra green areas in comparison (**Table 5.4.**).

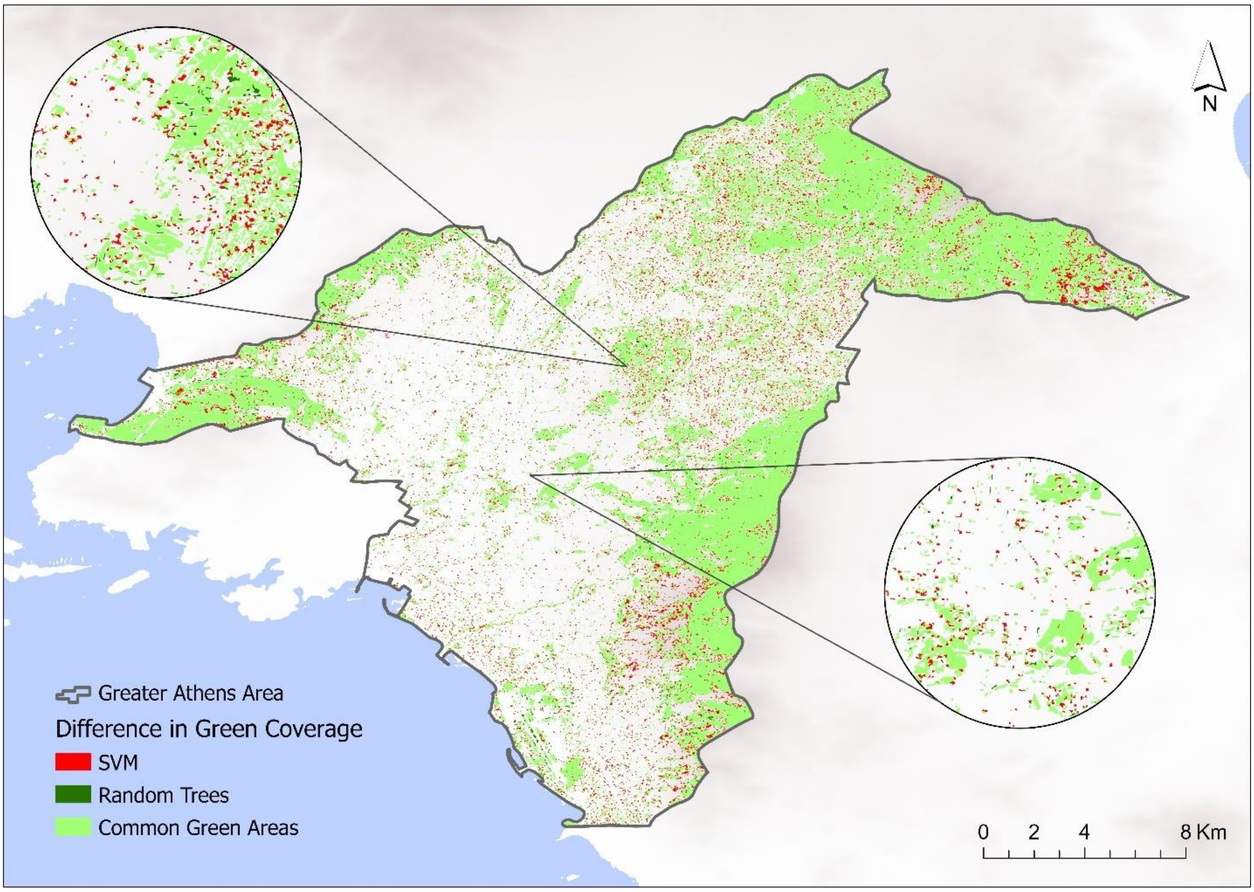

Figure 5.6. Symmetrical difference between the Random Trees and SVM classifiers on the Sentinel-2 imagery

Table 5.4.
Area comparison between Random Trees and SVM classifiers used on the Sentinel-2 imagery

Random Trees vs SVM (Sentinel-2)		
Extra in SVM	**Extra in RT**	**Common area**
18.1 km^2	2.71 km^2	115.21 km^2

5.3.3. PlanetScope vs Sentinel-2 with Random Trees

The Symmetrical Difference performed between the PlanetScope and Sentinel-2 imagery regarding the Random Trees classifier is presented in **Fig. 5.7.** The main differences are observed again in the mountainous areas, as well as in dry fields in the far north of the city. Within the urban fabric, the differences are fewer, yet still significant. The common green areas between them take up only 105.32 km^2 of land surface, while at the same time the PlanetScope image was classified as Green by 40.82 km^2 of extra land in comparison with the Sentinel-2, much more than the 12.59 km^2 of land that was classified as green in the Sentinel-2 image and not the PlanetScope one (**Table 5.5.**).

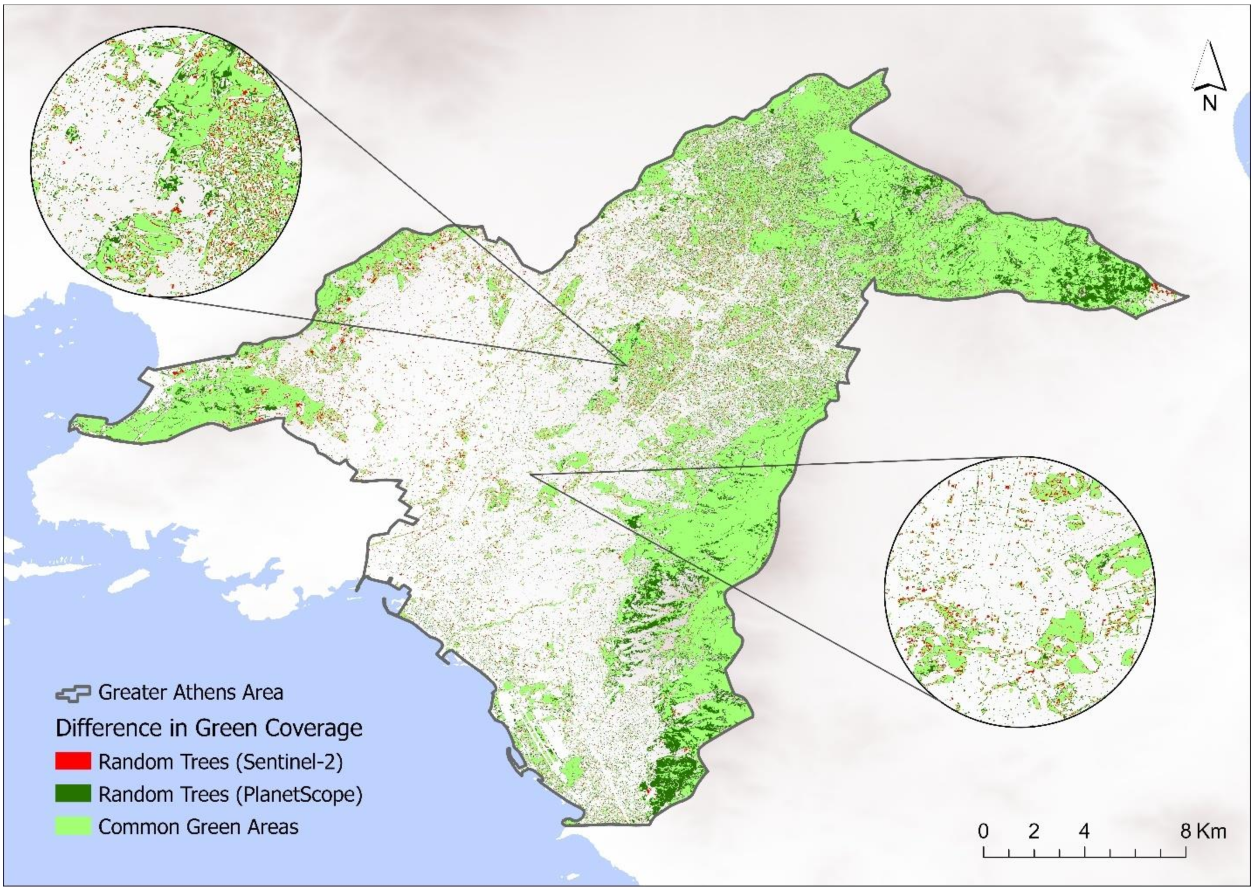

Figure 5.7. Symmetrical difference between PlanetScope and Sentinel-2 imagery on the Random Trees classifier

Table 5.5.
Area comparison between PlanetScope and Sentinel-2 imagery on the Random Trees classifier

PlanetScope vs Sentinel-2 (Random Trees)		
Extra in PS	**Extra in S2A**	**Common area**
40.82 km^2	12.59 km^2	105.32 km^2

5.3.4. PlanetScope vs Sentinel-2 with SVM

The Symmetrical Difference performed between the PlanetScope and Sentinel-2 imageries regarding the SVM classifier is presented in **Fig. 5.8.** The pattern is similar to the other dual comparisons made, with the biggest differences found in the mountain slopes and seemingly smaller but significant across the city. According to **Table 5.6.**, the common Green between the two images covers an area of 119.8 km^2. The PlanetScope imagery resulted in a lot more land classified as Green using the SVM classifier by 46.15 km^2 in relation to the Sentinel-2 imagery. In contrast, the Sentinel-2 image resulted in 13.53 km^2 of Green-classified land, that the PlanetScope image classified as Developed or Water.

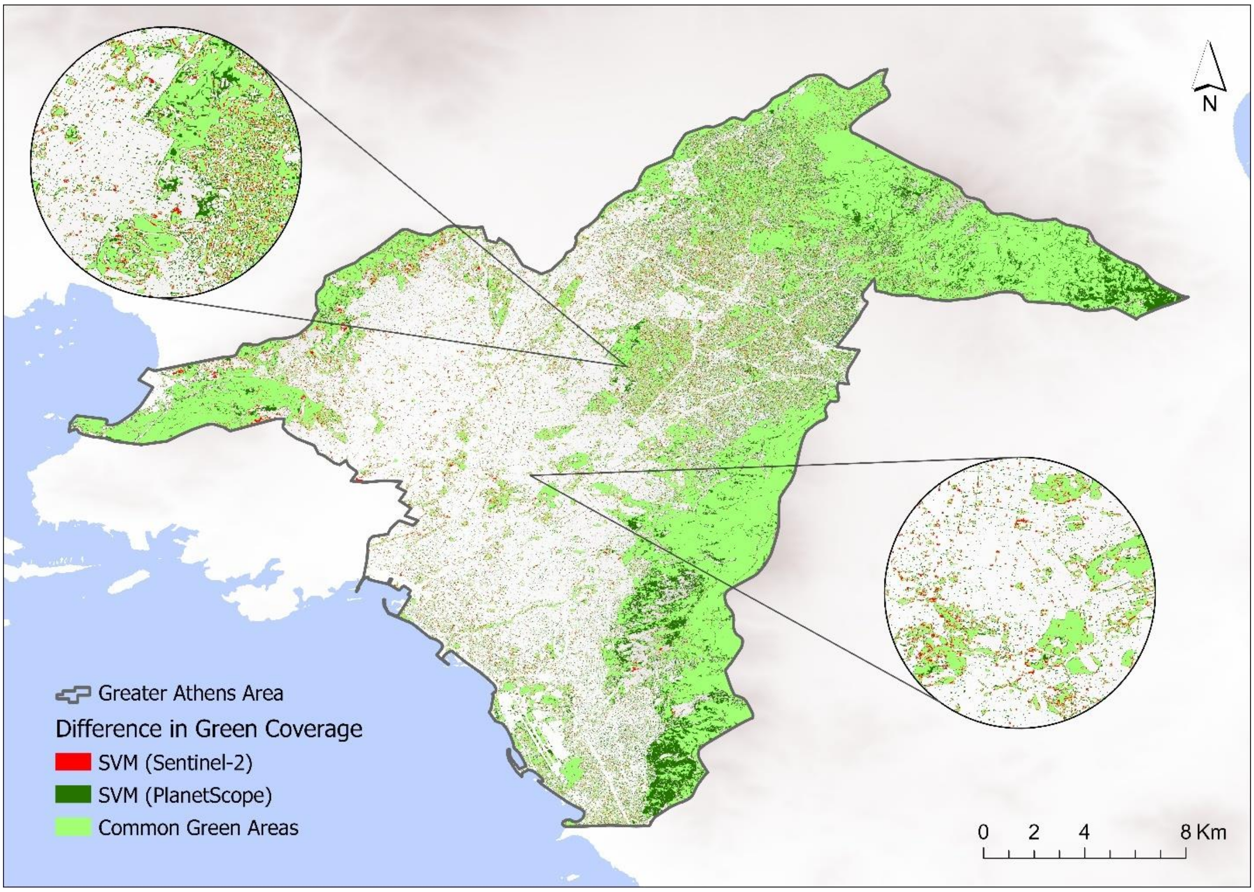

Figure 5.8. Symmetrical difference between PlanetScope and Sentinel-2 imagery on the SVM classifier

Table 5.6.
Area comparison between PlanetScope and Sentinel-2 imagery on the SVM classifier

PlanetScope vs Sentinel-2 (SVM)		
Extra in PS	**Extra in S2A**	**Common area**
46.15 km^2	13.53 km^2	119.8 km^2

5.4. Classification accuracy assessment results

The accuracy assessment carried out for the classification, resulted in the confusion (error) matrix shown in **Table 5.7**. It is evident that the techniques followed in the study's methodology attributed to very accurate results, for both the Random Trees and SVM algorithms and for either of PlanetScope and Sentinel-2 imagery. The overall accuracy ranged between 91% and 95%, the producer's accuracy between 87% and 100%, the user's accuracy between 83% and 97%. These high percentages reflect the high probability that the classification of each class corresponds to reality in the case of Producer's Accuracy, as well as the subjectivity and explicit selection of algorithm training samples by the user in the case of User's Accuracy.

Table 5.7.
Confusion (error) matrix of the Random Trees and SVM classification with 500 accuracy assessment points

	PlanetScope				Sentinel-2			
	Random Trees		Support Vector Machine		Random Trees		Support Vector Machine	
Class	**Producer's Accuracy (%)**	**User's Accuracy (%)**	**Producer's Accuracy (%)**	**User's Accuracy (%)**	**Producer's Accuracy (%)**	**User's Accuracy (%)**	**Producer's Accuracy (%)**	**User's Accuracy (%)**
Developed	92.73	96.96	89.77	97.93	97.2	91.75	92.71	92.39
Green	96.10	92.49	97.68	89.78	87.11	96.02	89.01	89.47
Water	100.00	83.33	100	86.95	100	95.24	100	95.24
Overall Accuracy (%)	**94.44**		**93.60**		**93.40**		**91.40**	
Kappa coefficient	**0.90**		**0.881**		**0.872**		**0.834**	

5.4.1. PlanetScope imagery

For the PlanetScope imagery, the Random Trees classification got an overall accuracy (OA) that reached 94.44%, while Cohen's kappa coefficient the value of 0.90. Regarding the classes' individual accuracy, the Producer's Accuracy ranges between 92.73% and 100%, while the User's Accuracy ranges between 83.33% and 96.96%. The low percentage on Water's UA is mostly due to the false classification of shadow and football fields with artificial turf that have a very similar spectral response with water surfaces.

The SVM classification of the PlanetScope image got a lower overall accuracy (OA) that reached 93.6%, as well as a lower Cohen's kappa coefficient with the value of 0.90. Regarding the classes' individual accuracy, the Producer's Accuracy ranges between 89.77% and 100%, while the User's Accuracy ranges between 86.95% and 97.93%.

The different sets of accuracy assessment points do not seem to reveal any specific pattern regarding the final accuracy of either of the two classifications **(Table 5.8.; Fig. 5.9.)**. The RT results are mostly similar, ranging between 91.5% and 94.48% on the OA and 0.843 to 0.906 on the K_c, with the exception of the set of 50 points, where the accuracy drops significantly to 84.2% OA and 0.749 K_c. On average, the OA is at 91.2% and the K_c at 0.850. The SVM results remain relatively unchanged, with small differences between each set of points. The OA and K_c remain above 91% and 0.83 respectively. The set of 25 points appears to have the highest OA at 97.06% and Kc at 0.955. The average OA is at 92.88% and the K_c at 0.875.

Table 5.8.
The OA and K_c results for a different number of accuracy assessment points for the classification of the PlanetScope image

	Random Trees		SVM	
Accuracy Assessment Points	Overall Accuracy (%)	Kappa coefficient	Overall Accuracy (%)	Kappa coefficient
25	91.17	0.866	97.05	0.955
50	84.21	0.749	91.22	0.859
100	94.34	0.902	91.50	0.854
250	91.60	0.845	91.20	0.838
400	91.47	0.843	92.73	0.866
500	94.40	0.896	93.60	0.881

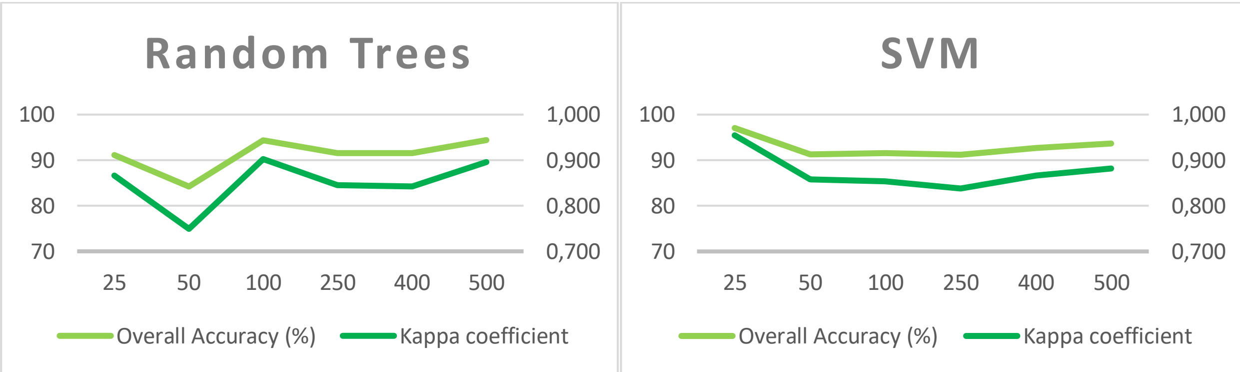

Figure 5.9. Graph depicting the Overall Accuracy and Kappa coefficient for five sets of a different number of accuracy assessment points for the classification of the PlanetScope image

5.4.2. Sentinel-2 imagery

For the Sentinel-2 imagery, the Random Trees classification got an overall accuracy (OA) that reached 93.4%, while Cohen's kappa coefficient the value of 0.872. Regarding the classes' individual accuracy, the Producer's Accuracy ranges between 87.11% and 100%, while the User's Accuracy ranges between 91.75% and 96.02%.

The SVM classification of the Sentinel-2 image got a lower overall accuracy (OA) that reached 91.4%, as well as a lower Kappa coefficient with the value of 0.834. Regarding the classes' individual accuracy, the Producer's Accuracy ranges between 89.01% and 100%, while the User's Accuracy ranges between 89.47% and 95.24%.

The different sets of accuracy assessment points in the case of the Sentinel-2 image seem to have some more variation in their results **(Table 5.9.; Fig. 5.10.)**. The accuracy of the RT results drops the fewer the points get until they reach 50 in number when it starts rising again, reaching the maximum OA and K_c at 100%. On average, the OA is at 91.58% and the K_c at 0.848. The SVM seems to have performed in a similar way, ranging between 88.6% and 100% on the OA and 0.819 to 1 on the K_c, with the lowest accuracy found in 50 points and the highest in 25. The average OA is at 92.51% and the K_c at 0.864.

Table 5.9.
OA and K_c results for a different number of accuracy assessment points for the classification of the Sentinel-2 image

	Random Trees		SVM	
Accuracy Assessment Points	Overall Accuracy (%)	Kappa coefficient	Overall Accuracy (%)	Kappa coefficient
25	100.00	1.000	100.00	1.000
50	91.22	0.858	91.22	0.858
100	85.84	0.752	88.60	0.802
250	87.60	0.765	90.40	0.819
400	91.47	0.843	93.48	0.876
500	93.40	0.871	91.40	0.834

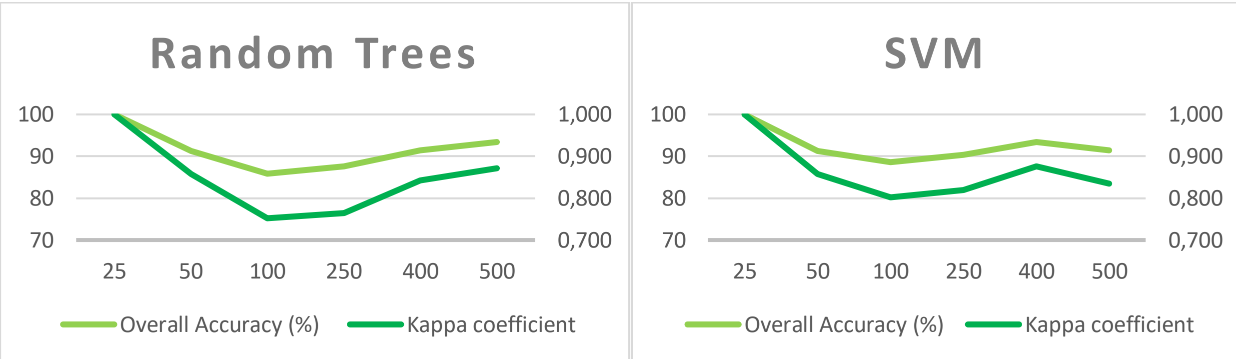

Figure 5.10. Graph depicting the Overall Accuracy and Kappa coefficient for five sets of a different number of accuracy assessment points for the classification of the PlanetScope image

5.5. Urban Atlas

The comparison of the city parks made between the Urban Atlas' class of Green Urban Areas and the Green areas that emerged from the classifications that were performed in the present analysis are shown in Figures **5.11.** and **5.12.** The two layers' difference in the surfaces characterized as "Green" is noticeably rather large, as there are polygons that have little to no common area between them. This is especially profound in cemeteries which are conceived as green spaces by Urban Atlas, when in reality their surface in most cases is covered mostly by pathways and tombstones, with very little vegetation around them. Other such cases are found on hills and parks with low vegetation or rocky surfaces. Polygons that appear to be more coherent than others are found mostly in the northeast of the study area where the landscape is generally forested.

In numbers, the GUAs cover an area of 22.1 km^2. In contrast, the classifications performed with the two classifiers on the two images resulted in an area as follows. For the PlanetScope imagery, the Random Trees classifier has a Green area of 14.98 km^2 bringing the non-common area to 7.1 km^2, while the SVM classifier has a slightly higher Green area of 16 km^2 reducing the extension of the non-common area to 6.09 km^2. For the Sentinel-2 imagery, the common area is yet lower compared to the PlanetScope imagery. The Random Trees classifier resulted in a common Green area of 14.37 km^2, therefore bringing the non-common area up to 7.73 km^2. The SVM classifier has a larger surface of common Green areas in this case too, at 15.07 km^2, while the non-common area is at 7.03 km^2.

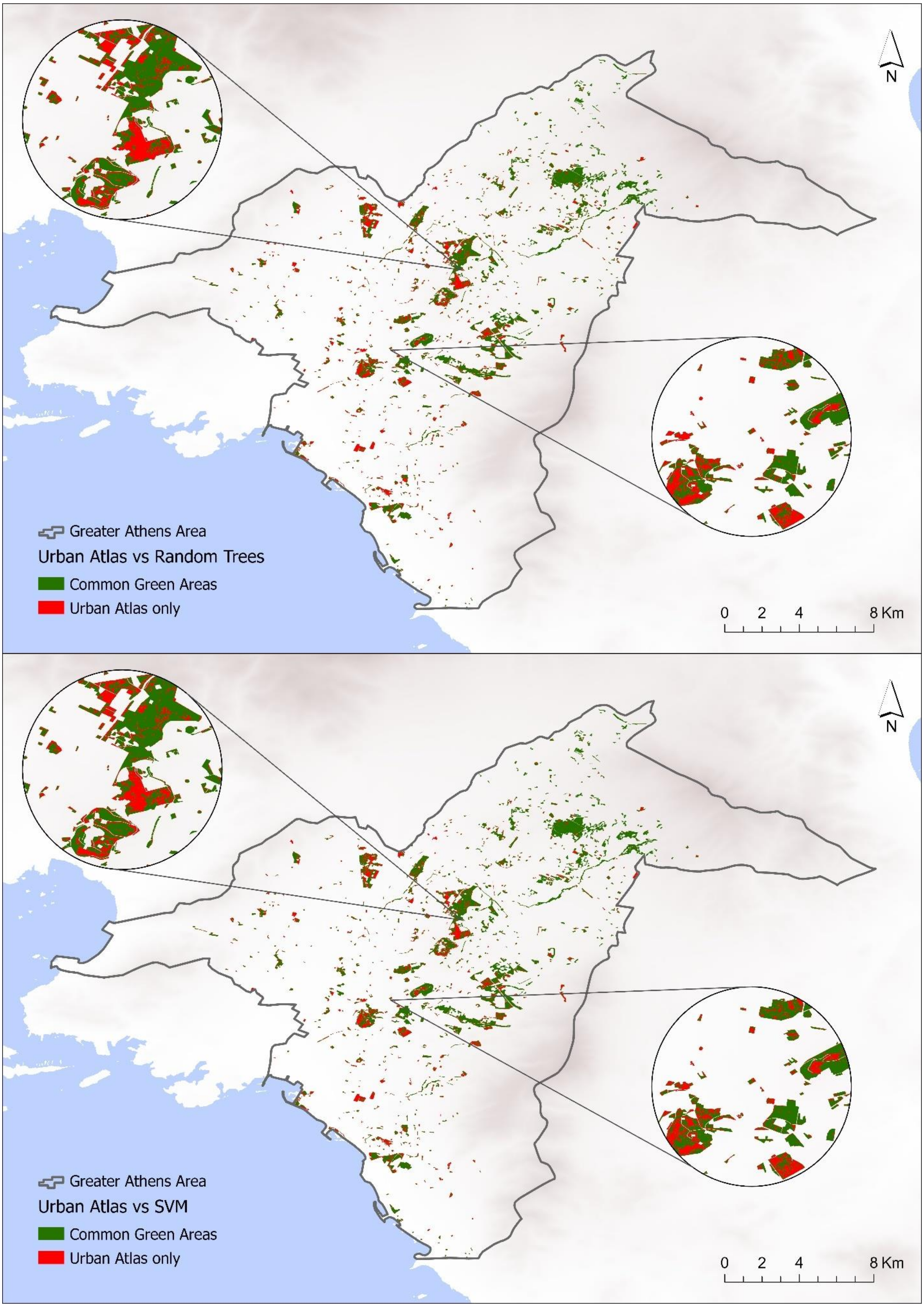

Figure 5.11. The Green Spaces that emerged from the Random Trees and SVM classifications on the PlanetScope image were clipped with the Urban Atlas class of Urban Green Areas. The red color represents the surfaces classified as Green Spaces by UA but as Developed by the methodology followed in the study.

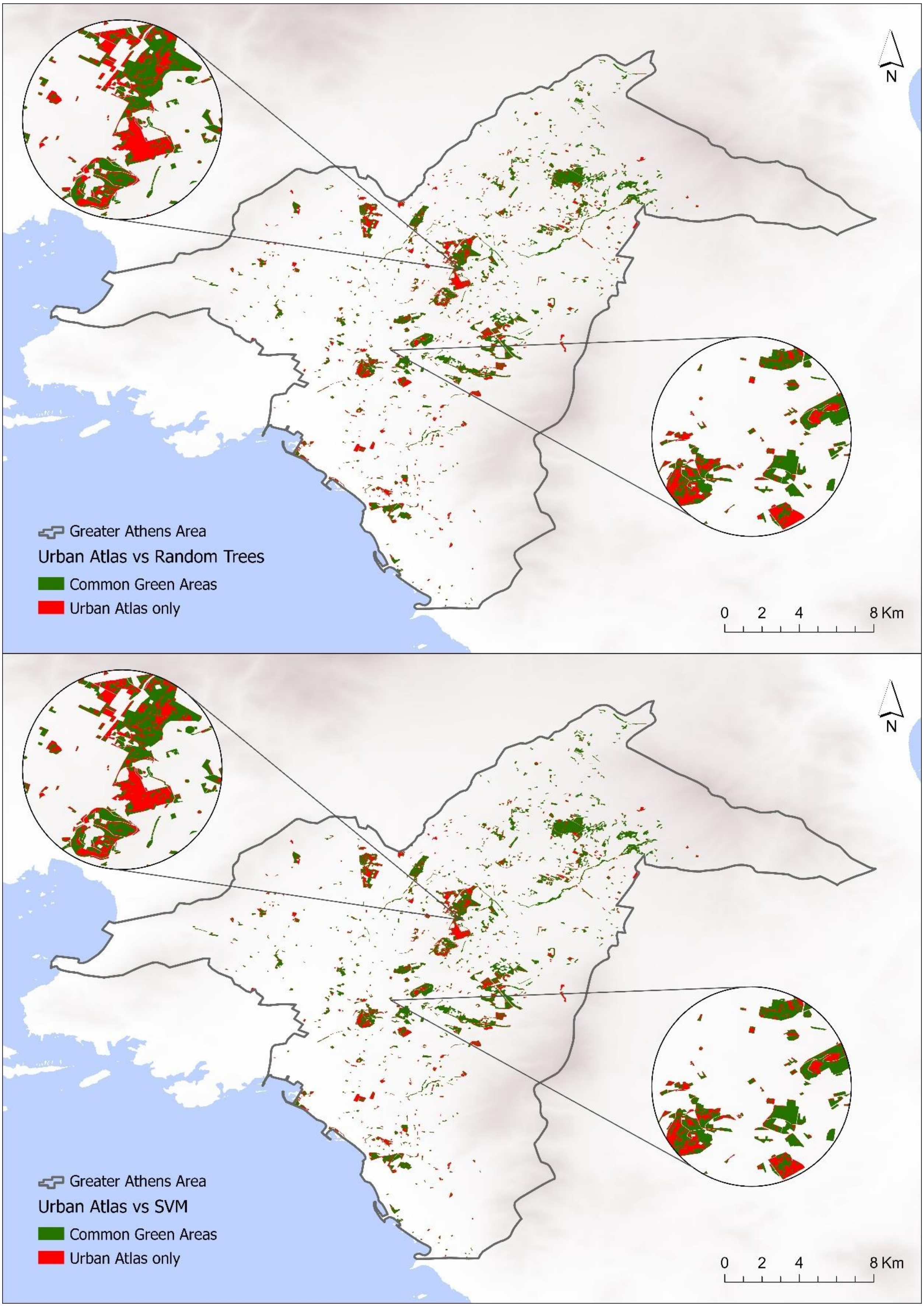

Figure 5.12. The Green Spaces that emerged from the Random Trees and SVM classifications on the Sentinel-2 image were clipped with the Urban Atlas class of Urban Green Areas. The red color represents the surfaces classified as Green Spaces by UA but as Developed by the methodology followed in the study.

Chapter 6: Discussion

In the present study, the GEOBIA method was implemented with very high spatial resolution imagery from PlanetScope and medium spatial resolution imagery from Sentinel-2 to extract urban green spaces for the Greater Athens Area, in Greece. This method, in addition to the spectral information recorded at the image pixels, includes as well the implementation of a segmentation of the image that allows the generation of objects with spectrally and texturally homogeneous characteristics. As such, those methods generally tend to produce better visually and more accurate results in comparison to pixel-based classifiers (Petropoulos et al., 2012b; 2015; Pandey et al., 2020). In the present study, OBIA returned very satisfactory results for the experimental study it was implemented for, as it is suggested from the statistical metrics that were computed and also the comparisons versus the Urban Green Atlas product. Results reported herein are comparable to those reported in other studies also using the GEOBIA technique with remote sensing multispectral imagery (Zylshal et al., 2016; Ozlem Yilmaz et al., 2019; Al-Doski, et al., 2020; Topaloğlu et al., 2021).

This chapter intends to cover the limitations of the methods and datasets used in the present study.

6.1. Segmentation limitations

The potential error sources in the technical implementation in this study affecting the technique's performance may be attributed to many possible reasons. For example, segmentation parameterization can be very challenging and lead to quite different results when they are not applied correctly. An over-segmentation leads to an excessive number of objects with different spectral responses and, in combination with a low number of training samples, can negatively impact the classification's accuracy (Pandey et al., 2020). On the other hand, an under-segmentation can lead to very homogeneous objects that incorporate the spectral response from different classes, thus also having a negative impact on the classification's accuracy (Elatawneh et al., 2012; Dawson et al., 2019). This issue has been solved by testing several values for the scale parameter in the segmentation process and choosing the appropriate one. This process can be automated by using an algorithm that calculates the local variance for the objects generated with a specific scale parameter offering information on the slightest changes in the segmentation process (Drăguţ et al., 2010; Drăguţ et al., 2014).

6.2. Sensor-related differences

Another possible reason might be related to the spectral characteristics of the urban green spaces and their spectral similarity to other objects also present in the images. For example, there are several studies that reported that the presence of numerous spectrally unique and ambiguous materials such as dark shingles and asphalt roads that makes their discrimination and consequently classification process slightly inaccurate (Petropoulos et al., 2015; Fragou et al., 2020). The results revealed a great difference in the extension of the green areas among the two images across the city. PlanetScope resulted overall in a much higher ratio of green spaces than Sentinel-2. The same is also true for the SVM in comparison with the Random Trees classifier in both images. The majority of those differences were located on the mountain slopes where there is low vegetation that emerged after several wildfires in recent years. A similar situation is observed in empty land plots across the city, especially in suburban areas. Due to the summer season, the images were retrieved for and the lack of rainfall, low vegetation completely dried up. The spectral response of those areas was regarded as green by PlanetScope, whereas Sentinel's spectral resolution differentiated the dry vegetation from the live one and therefore classified it as developed.

In some instances, shadows were also misinterpreted as vegetation. The tree canopy and the satellites' viewing angle posed difficulties for the segmentation and later the classification, as the 3-meter and 10-meter pixel resolutions were not clear enough to allow the algorithms to tell such details apart. This issue was exacerbated even further by the 10-meter pixel resolution of the Sentinel-2 imagery. Despite the fact that Sentinel-2 is ideal for monitoring plant growth, as well as for mapping changes in land cover and monitoring the world's forests (ESA, 2022), in cases of urban green mapping the analysis gets trickier, as the spatial analysis of 10 meters impedes the detailed recording of smaller green spaces. PlanetScope imagery may lack spectral resolution in comparison, however, the most important for UGSs mapping is a higher spatial resolution.

Another tricky feature for the classifiers, particularly in the case of PlanetScope, is the tiled roofs that in many cases were classified as vegetation. In addition, some buildings and open spaces are covered by spectrally similar urban surface materials, which further hamper clear discrimination between them. Other factors that may further complicate the analysis of urban areas leading to high within-class spectral variability include the 3-dimensional heterogeneity of urban areas and urban vegetation cover material aging (Herold & Roberts, 2005).

All the above reasons lead to the conclusion that a further spectral separability analysis would be appropriate to be implemented on the training samples to avoid as much as possible such errors. One such method, that is not available in ArcGIS but could be performed in ENVI, is the Jeffries-Matusita distance method, according to which inter-class spectral separability is calculated in the classification scheme. The closer the distance or separation between classes, the more the two classes are vulnerable to being misclassified and vice versa (Wicaksono & Aryaguna, 2020).

6.3. Classifiers' parametrization

Another important factor that should be taken into account is the lack of parametrization that is provided by the ArcGIS Pro tools, especially the ones related to the classifiers. The tools provided by the software lack of parametrization choices which are mostly set in default, such as the kernel type in the case of SVM, in an effort to provide a more user-friendly environment. Nevertheless, they proved to be highly effective in classifying satellite imagery compared, yet probably not equally accurate compared with other software tools that are intended for processing EO data, like ENVI and eCognition. The presence of parametrization choices would allow the examination of different alternatives of the algorithms and possibly lead to better results.

6.4. Urban Atlas limitations

Furthermore, a possible reason for the difference between the GEOBIA and the Urban Atlas layers is that the UA classifies the land according to its land use and treats each object as one whole entity (European Commission, 2020). Surfaces within parks where paths, open squares, bare soil, or rocks are found are not presented as such. Another example would be the cemeteries that are classified as GUA as a whole by UA, though, it is obvious that they are not completely covered by vegetation. On the contrary, the classification performed in this study shows the land cover rather than the land use. As a result, impermeable surfaces within green urban areas were classified as developed, therefore not matching 100% with the UA. Moreover, even if both data sources of UA and PlanetScope have similar resolutions (3m for Planet Scope images and 2-4m for the different images used to derivate the UA), the minimum mapping width of 10m used for Urban Atlas excludes linear elements which separate different elements from the same class (e.g., roads and street trees). The Sentinel-2 imagery partly exacerbates this difference due to its lower spatial resolution.

6.5. Classification accuracy

Regarding the classification accuracy, it refers to the degree of agreement between reality and the classified image. A thematic classification map is considered accurate when it provides an objective representation of the land cover of the area it depicts (Foody, 2002). According to Foody (2004), accuracy assessment is necessary for a classification to be considered complete, as many inaccuracies are often identified. In this application, with an overall accuracy of over 90% for all four cases, the classification was expressed with very high accuracy and can be considered successful.

According to Lillesand et al. (2015), a minimum of 50 validation points should be obtained per landcover class. In that sense, for the 3 landcover classes of this study, and considering that the analysis was performed on a large area, a minimum of 400 validation points would be required in total. It should be noted, though, that the extension of each landcover class may also determine the number of validation points that correspond to them when using random stratified sampling. Therefore, it is safe to say the 400 and 500 validation points provided better and more credible validation results.

Chapter 7: Conclusions and future work

The study's main objective was to implement the GEOBIA method and the Random Trees and SVM classifiers to classify and extract the green urban areas of Athens, using PlanetScope and Sentinel-2 imagery. The innovative aspect of this study is found in the use of and comparison of the two datasets as well as the comparison of the two classifiers and the validation of the results with the Urban Atlas. Overall, the results confirmed the research findings in the literature about the great utility of the method and the high overall and individual accuracy of the classes obtained by selecting only a small sample of objects for the training regions.

PlanetScope proved to be ideal for applications that require high-resolution imagery, as it provides free and already pre-processed data for developers but not for commercial use. On the same note, Sentinel-2 is greatly useful in a vast variety of applications as it provides free, multispectral data in pre-processed or raw versions. In the analysis, the Sentinel-2 image showed more variation in terms of the pixels' spectral response, which makes the satellite more suitable in cases when the image is required to be classified into further classes and make distinctions over the specific vegetation types. Nevertheless, this can't undermine the great utility of PlanetScope's high spatial resolution imagery, which proved to be of essential importance for the study of urban areas. This is especially true for densely built-up cities like Athens, where the detail of an HSR image helps in better classifying the different classes. Sentinel's 10 m spatial resolution made the validation of the results much harder, as different spectral identities were mixed up in each pixel in these compact areas.

When it comes to the classifiers used in the analysis, Random Trees outperformed SVM in terms of its accuracy in both imageries. Support Vector Machine is a supervised learning model which is probably the most popular in classification challenges. However, it is mostly used in classification problems where the data is sparse and easy to classify. Random Forest is one of the most used classifications in machine learning and has been gaining even more popularity in recent years in classification tasks, with its implementation exceeding the SVM method (Sheykhmousa et al., 2020). According to a review on SVM vs RF for remote sensing image classification by Sheykhmousa et al. (2020), the classification accuracies of the classifiers showed high variations, however, when it comes to land use – land cover applications the variance of Random Forest was little, showing its superiority over SVM on this field.

The core of the city of Athens was confirmed to have very few UGSs of substantial size, especially in the case of excluding hilly and mountainous areas. One limitation of this study is that the extracted green areas include the trees' canopy which may cover impermeable types of land cover. In this case, the exact size of the specific cover types is not precise and extra work needs to be done in order to deal with this overlapping.

The Urban Atlas is a valuable dataset that can be used in various applications. However, many of its classes, aside from the initial classification, have received further manual work, emitting land cover types that are contained within larger ones. This is the case with the UGSs, where impermeable land cover types like paved paths, squares, or even tombs in cemeteries were absorbed in the larger UGSs class. Therefore, its use as reference data for accuracy assessment should be taken with a grain of salt.

In a broader context, the results of the present study may provide an important contribution toward the implementation of successful urban landscape planning and infrastructure development. The potential of this method's operationalization may act as added value in the direction of improving existing global operational products, such as Urban Atlas. High-resolution imagery was proven to be more successful in classifying urban green, than medium-resolution imagery. On that account, PlanetScope or any other HSR imagery distributor is more suitable for such studies that require detail despite the possible costs. Last but not least, the findings of the present study can support global studies ongoing towards the evaluation of the capability of PlanetScope imagery use in obtaining UGSs, potentially at an operational scale.

All in all, GEOBIA is a robust and perhaps more cumbersome to implement in comparison to most pixel-based classifiers, resulting generally also to more accurate classification results. Several studies have shown that only good segmentation results can lead to object-oriented image classification outperforming pixel-based classification (Pandey et al., 2020). Thus, the user experience with the GEOBIA implementation is a factor to be taken into account. On a positive note, the technique, at least in the present case study, did not require significant computational resources in its implementation, which can be important if access to such resources is limited.

7.1. Future research

In this section, potential research recommendations are mentioned that need pursuing for the further expansion of the present study in addressing and improving our understanding of the quality, quantity, and future needs of the UGSs in the city of Athens.

1. Further classification of the green areas in more specific vegetation types, i.e., trees, sclerophyllous vegetation, and low vegetation. This could provide a better picture of how functional these spaces are, as low vegetation areas such as empty building plots are highly changeable and do not offer much in ecosystem services.
2. Examination of the plants' health in order to determine the amount of the green spaces that have a substantial positive effect on the overall quality of life in the city.
3. Study of the different ecosystem services the examined green areas provide the city's residents with.
4. Focus on the study of the small UGSs and their contribution to mitigating the negative effects that surround the city's intense urbanization.

References

Adankon, M. M., & Cheriet, M. (2009). Support Vector Machine. *Encyclopedia of Biometrics*, 1303–1308. https://doi.org/10.1007/978-0-387-73003-5_299

Al-Doski, J., Mansor, S. B., & Khuzaimah, Z. (2020). Land Cover Mapping Using Remote Sensing Data. *American Journal of Geographic Information System*, *9*(1), 33–45. https://doi.org/10.5923/j.ajgis.20200901.04

Amini, S., Homayouni, S., Safari, A., & Darvishsefat, A. A. (2018). Object-based classification of hyperspectral data using Random Forest algorithm. *Geo-Spatial Information Science*, *21*(2), 127–138. https://doi.org/10.1080/10095020.2017.1399674

Burkhard, B., & Maes, J. (2017). *Mapping Ecosystem Services*. Pensoft.

Cass, A., Petropoulos, G. P., Ferentinos, K. P., Pavlides, A., & Srivastava, P. K. (2019). Exploring the synergy between Landsat and ASAR towards improving thematic mapping accuracy of optical EO data. *Applied Geomatics*, *11*(3), 277–288. https://doi.org/10.1007/s12518-019-00258-7

Chen, B., Nie, Z., Chen, Z., & Xu, B. (2017). Quantitative estimation of 21st-century urban greenspace changes in Chinese populous cities. *Science of The Total Environment*, *609*, 956–965. https://doi.org/10.1016/j.scitotenv.2017.07.238

Cheng, Y. D., Farmer, J. R., Dickinson, S. L., Robeson, S. M., Fischer, B. C., & Reynolds, H. L. (2021). Climate change impacts and urban green space adaptation efforts: Evidence from U.S. municipal parks and recreation departments. *Urban Climate*, *39*, 100962. https://doi.org/10.1016/j.uclim.2021.100962

Chorianopoulos, I., Pagonis, T., Koukoulas, S., & Drymoniti, S. (2010). Planning, competitiveness and sprawl in the Mediterranean city: The case of Athens. Cities, 27(4), 249–259. https://doi.org/10.1016/j.cities.2009.12.011

Churches, C. E., Wampler, P. J., Sun, W., & Smith, A. J. (2014). Evaluation of forest cover estimates for Haiti using supervised classification of Landsat data. *International Journal of Applied Earth Observation and Geoinformation*, *30*, 203–216. https://doi.org/10.1016/j.jag.2014.01.020

Climatic Data for Nea Filadefia station (2022). Hellenic National Meteorological Service. http://emy.gr/emy/en/climatology/climatology_city

Colding, J., Gren, S., & Barthel, S. (2020). The Incremental Demise of Urban Green Spaces. *Land*, *9*(5), 162. https://doi.org/10.3390/land9050162

Congalton, R. G. (1991). A review of assessing the accuracy of classifications of remotely sensed data. *Remote Sensing of Environment*, *37*(1), 35–46. https://doi.org/10.1016/0034-4257(91)90048-b

Copernicus Open Access Hub (2022). European Space Agency. https://scihub.copernicus.eu/

Copernicus Programme (2021). Validation Services for the geospatial products of the Copernicus land Continental and local components including in-situ data. Issue 1.6. https://land.copernicus.eu/user-corner/technical-library/urban-atlas-2018-validation-report

Dadvand, P., Bartoll, X., Basagaña, X., Dalmau-Bueno, A., Martinez, D., Ambros, A., Cirach, M., Triguero-Mas, M., Gascon, M., Borrell, C., & Nieuwenhuijsen, M. J. (2016). Green spaces and General Health: Roles of mental health status, social support, and physical activity. Environment International, 91, 161–167. https://doi.org/10.1016/j.envint.2016.02.029

Dawson, R. A., Petropoulos, G. P., Toulios, L., & Srivastava, P. K. (2019). Mapping and monitoring of the land use/cover changes in the wider area of Itanos, Crete, using very high resolution EO imagery with specific interest in archaeological sites. *Environment, Development and Sustainability*, *22*(4), 3433–3460. https://doi.org/10.1007/s10668-019-00353-0

Degerickx, J., Hermy, M., & Somers, B. (2020). Mapping Functional Urban Green Types Using High Resolution Remote Sensing Data. *Sustainability*, *12*(5), 2144. https://doi.org/10.3390/su12052144

Dhingra, S., & Kumar, D. (2019). A review of remotely sensed satellite image classification. *International Journal of Electrical and Computer Engineering (IJECE)*, *9*(3), 1720. https://doi.org/10.11591/ijece.v9i3.pp1720-1731

Dosiadis, E., Triantakonstantis, D., Popa, A. M., Detsikas, S. E., Sandric, I., Petropoulos, G. P., Onose, D., & Chalkias, C. (2022a). A GEOBIA-based approach for mapping Urban Green Spaces using PlanetScope imagery: the case of Athens. EGU General Assembly 2022. https://doi.org/10.5194/egusphere-egu22-11946

Dosiadis, E., Petropoulos, G. P., Popa, A. M., Sandric, I., Faka, A., Onose, D., & Srivastava, P. (2022b). Using PlanetScope imagery and GEOBIA to map urban green spaces. Earth Observation in Urban Monitoring: Techniques and Challenges.

Drăguţ, L., Csillik, O., Eisank, C., & Tiede, D. (2014). Automated parameterization for multi-scale image segmentation on multiple layers. *ISPRS Journal of Photogrammetry and Remote Sensing*, *88*, 119–127. https://doi.org/10.1016/j.isprsjprs.2013.11.018

Drăguţ, L., Tiede, D., & Levick, S. R. (2010). ESP: a tool to estimate scale parameter for multiresolution image segmentation of remotely sensed data. *International Journal of Geographical Information Science*, *24*(6), 859–871. https://doi.org/10.1080/13658810903174803

Elatawneh, A., Kalaitzidis, C., Petropoulos, G. P., & Schneider, T. (2012a). Evaluation of diverse classification approaches for land use/cover mapping in a Mediterranean region utilizing Hyperion data. *International Journal of Digital Earth*, *7*(3), 194–216. https://doi.org/10.1080/17538947.2012.671378

Elatawneh, A., Kalaitzidis, C., Petropoulos, G. P., & Schneider, T. (2012b). Evaluation of diverse classification approaches for land use/cover mapping in a Mediterranean region utilizing Hyperion data. *International Journal of Digital Earth*, *7*(3), 194–216. https://doi.org/10.1080/17538947.2012.671378

ESRI (2022a). Segment Mean Shift (Image Analyst)—ArcGIS Pro | Documentation. https://pro.arcgis.com/en/pro-app/latest/tool-reference/image-analyst/segment-mean-shift.htm

ESRI (2022b). Train Random Trees Classifier (Image Analyst)—ArcGIS Pro | Documentation. https://pro.arcgis.com/en/pro-app/latest/tool-reference/image-analyst/train-random-trees-classifier.htm

European Commission (2020). Mapping Guide for a European Urban Atlas Regional Policy. https://land.copernicus.eu/user-corner/technical-library/urban_atlas_2012_2018_mapping_guide

European Commission. Directorate-General for the Environment. (2013). *Mapping and Assessment of Ecosystems and Their Services*. Publications Office. https://doi.org/10.2779/12398

Feltynowski, M., Kronenberg, J., Bergier, T., Kabisch, N., ŁAszkiewicz, E., & Strohbach, M. W. (2018). Challenges of urban green space management in the face of using inadequate data. *Urban Forestry & Urban Greening*, *31*, 56–66. https://doi.org/10.1016/j.ufug.2017.12.003

Feng, Q., Liu, J., & Gong, J. (2015). UAV Remote Sensing for Urban Vegetation Mapping Using Random Forest and Texture Analysis. *Remote Sensing*, *7*(1), 1074–1094. https://doi.org/10.3390/rs70101074

Ferreira, F., Vasconcelos, L., & Ferreira, J. C. (2022). Socio-ecological and economic evaluation of urban parks - A methodology integrating and articulating diverse components. Journal of Outdoor Recreation and Tourism, 100512. https://doi.org/10.1016/j.jort.2022.100512

Foody, G. M. (2002). Status of land cover classification accuracy assessment. *Remote Sensing of Environment*, *80*(1), 185–201. https://doi.org/10.1016/s0034-4257(01)00295-4

Foody, G. M. (2004). Thematic Map Comparison. *Photogrammetric Engineering & Remote Sensing*, *70*(5), 627–633. https://doi.org/10.14358/pers.70.5.627

Fragou, S., Kalogeropoulos, K., Stathopoulos, N., Louka, P., Srivastava, P. K., Karpouzas, S., P. Kalivas, D., & P. Petropoulos, G. (2020). Quantifying Land Cover Changes in a Mediterranean Environment Using Landsat TM and Support Vector Machines. *Forests*, *11*(7), 750. https://doi.org/10.3390/f11070750

Gaitani, N., Spanou, A., Saliari, M., Synnefa, A., Vassilakopoulou, K., Papadopoulou, K., Pavlou, K., Santamouris, M., Papaioannou, M., & Lagoudaki, A. (2011). Improving the microclimate in urban areas: a case study in the center of Athens. Building Services Engineering Research and Technology, 32(1), 53–71. https://doi.org/10.1177/0143624410394518

García-Gonzalo, E., Fernández-Muñiz, Z., García Nieto, P., Bernardo Sánchez, A., & Menéndez Fernández, M. (2016). Hard-Rock Stability Analysis for Span Design in Entry-Type Excavations with Learning Classifiers. Materials, 9(7), 531. https://doi.org/10.3390/ma9070531

Ghahramani, M., Galle, N. J., Ratti, C., & Pilla, F. (2021). Tales of a city: Sentiment analysis of urban green space in Dublin. *Cities*, *119*, 103395. https://doi.org/10.1016/j.cities.2021.103395

Glasgow, G. (2005). Stratified Sampling Types. *Encyclopedia of Social Measurement*, 683–688. https://doi.org/10.1016/b0-12-369398-5/00066-9

Gülçin, D., & Akpınar, A. (2018). Mapping Urban Green Spaces Based on an Object-Oriented Approach. *Bilge International Journal of Science and Technology Research*, *2*, 71–81. https://doi.org/10.30516/bilgesci.486893

Haas, J., & Ban, Y. (2017). Sentinel-1A SAR and sentinel-2A MSI data fusion for urban ecosystem service mapping. *Remote Sensing Applications: Society and Environment*, *8*, 41–53. https://doi.org/10.1016/j.rsase.2017.07.006

Haines-Young, R., & Potschin-Young, M. (2018). Revision of the Common International Classification for Ecosystem Services (CICES V5.1): A Policy Brief. *One Ecosystem*, *3*, e27108. https://doi.org/10.3897/oneeco.3.e27108

Hay, G. J., & Castilla, G. (2008). Geographic Object-Based Image Analysis (GEOBIA): A new name for a new discipline. *Lecture Notes in Geoinformation and Cartography*, 75–89. https://doi.org/10.1007/978-3-540-77058-9_4

Herold, M., & Roberts, D. (2005). Spectral characteristics of asphalt road aging and deterioration: implications for remote-sensing applications. *Applied Optics*, *44*(20), 4327. https://doi.org/10.1364/ao.44.004327

Hossain, M. D., & Chen, D. (2019). Segmentation for Object-Based Image Analysis (OBIA): A review of algorithms and challenges from remote sensing perspective. *ISPRS Journal of Photogrammetry and Remote Sensing*, *150*, 115–134. https://doi.org/10.1016/j.isprsjprs.2019.02.009

Huerta, R. E., Yépez, F. D., Lozano-García, D. F., Guerra Cobián, V. H., Ferriño Fierro, A. L., de León Gómez, H., Cavazos González, R. A., & Vargas-Martínez, A. (2021). Mapping Urban Green Spaces at the Metropolitan Level Using Very High Resolution Satellite Imagery and Deep Learning Techniques for Semantic Segmentation. *Remote Sensing*, *13*(11), 2031. https://doi.org/10.3390/rs13112031

Ikokou, G. B., & Smit, J. (2021). Optimal segmentation parameters prediction using a orthogonal decomposition approach for geographical object based classification of urban areas. *The Egyptian Journal of Remote Sensing and Space Science*, *24*(3), 501–507. https://doi.org/10.1016/j.ejrs.2021.04.001

Javadi, R., & Nasrollahi, N. (2021). Urban green space and health: The role of thermal comfort on the health benefits from the urban green space; a review study. *Building and Environment*, *202*, 108039. https://doi.org/10.1016/j.buildenv.2021.108039

Jennings, V., & Bamkole, O. (2019). The Relationship between Social Cohesion and Urban Green Space: An Avenue for Health Promotion. International Journal of Environmental Research and Public Health, 16(3), 452. https://doi.org/10.3390/ijerph16030452

Kartalis, K., & Feidas, Ch. (2015). Αρχές και Εφαρμογές Δορυφορικής Τηλεπισκόπησης. [Principles and Applications of Satellite Remote Sensing]. Tziolas Publications. ISBN 978-960-418-401-9

Kassomenos, P., Kissas, G., Petrou, I., Begou, P., Khan, H. S., & Santamouris, M. (2022). The influence of daily weather types on the development and intensity of the urban heat island in two Mediterranean coastal metropolises. *Science of The Total Environment*, *819*, 153071. https://doi.org/10.1016/j.scitotenv.2022.153071

Kassomenos, P., Kissas, G., Petrou, I., Begou, P., Khan, H. S., & Santamouris, M. (2022). The influence of daily weather types on the development and intensity of the urban heat island in two Mediterranean coastal metropolises. Science of The Total Environment, 819, 153071. https://doi.org/10.1016/j.scitotenv.2022.153071

Khan, M. Y., Qayoom, A., Nizami, M. S., Siddiqui, M. S., Wasi, S., & Raazi, S. M. K. U. R. (2021). Automated Prediction of Good Dictionary EXamples (GDEX): A Comprehensive Experiment with Distant Supervision, Machine Learning, and Word Embedding-Based Deep Learning Techniques. Complexity, 2021, 1–18. https://doi.org/10.1155/2021/2553199

Kolcsár, R. A., Csikós, N., & Szilassi, P. (2021a). Testing the limitations of buffer zones and Urban atlas population data in urban green space provision analyses through the case study of Szeged, Hungary. *Urban Forestry & Urban Greening*, *57*, 126942. https://doi.org/10.1016/j.ufug.2020.126942

Kolcsár, R. A., Csikós, N., & Szilassi, P. (2021b). Testing the limitations of buffer zones and Urban atlas population data in urban green space provision analyses through the case study of Szeged, Hungary. *Urban Forestry & Urban Greening*, *57*, 126942. https://doi.org/10.1016/j.ufug.2020.126942

Kopecká, M., Szatmári, D., & Rosina, K. (2017). Analysis of Urban Green Spaces Based on Sentinel-2A: Case Studies from Slovakia. Land, 6(2), 25. https://doi.org/10.3390/land6020025

Kourtidis, K., Georgoulias, A., Rapsomanikis, S., Amiridis, V., Keramitsoglou, I., Hooyberghs, H., Maiheu, B., & Melas, D. (2015). A study of the hourly variability of the urban heat island effect in the Greater Athens Area during summer. *Science of The Total Environment*, *517*, 162–177. https://doi.org/10.1016/j.scitotenv.2015.02.062

Kumar, P. (Ed.). (2011). The Economics of Ecosystems and Biodiversity: Ecological and Economic Foundations (1st ed.). Routledge. https://doi.org/10.4324/9781849775489

Lahoti, S., Kefi, M., Lahoti, A., & Saito, O. (2019). Mapping Methodology of Public Urban Green Spaces Using GIS: An Example of Nagpur City, India. *Sustainability*, *11*(7), 2166. https://doi.org/10.3390/su11072166

Lau, K. K. L., Yung, C. C. Y., & Tan, Z. (2021). Usage and perception of urban green space of older adults in the high-density city of Hong Kong. *Urban Forestry & Urban Greening*, *64*, 127251. https://doi.org/10.1016/j.ufug.2021.127251

Law 4280/2014: Environmental upgrade and private urban planning - Sustainable development of settlements - Regulations of forest legislation and other provisions (2014). Greek Ministry of Environment and Energy. http://www.opengov.gr/minenv/?p=5470

Lebourgeois, V., Dupuy, S., Vintrou, L., Ameline, M., Butler, S., & Bégué, A. (2017). A Combined Random Forest and OBIA Classification Scheme for Mapping Smallholder Agriculture at Different Nomenclature Levels Using Multisource Data (Simulated Sentinel-2 Time Series, VHRS and DEM). *Remote Sensing*, *9*(3), 259. https://doi.org/10.3390/rs9030259

Li, M., Zang, S., Zhang, B., Li, S., & Wu, C. (2014). A Review of Remote Sensing Image Classification Techniques: the Role of Spatio-contextual Information. *European Journal of Remote Sensing*, *47*(1), 389–411. https://doi.org/10.5721/eujrs20144723

Lillesand, T., Kiefer, R. W., & Chipman, J. (2015). *Remote Sensing and Image Interpretation*. Wiley.

Liu, D., & Xia, F. (2010). Assessing object-based classification: advantages and limitations. Remote Sensing Letters, 1(4), 187–194. https://doi.org/10.1080/01431161003743173

Liu, J., Zhang, L., Zhang, Q., Li, C., Zhang, G., & Wang, Y. (2022). Spatiotemporal evolution differences of urban green space: A comparative case study of Shanghai and Xuchang in China. *Land Use Policy*, *112*, 105824. https://doi.org/10.1016/j.landusepol.2021.105824

Lu, D., & Weng, Q. (2007). A survey of image classification methods and techniques for improving classification performance. *International Journal of Remote Sensing*, *28*(5), 823–870. https://doi.org/10.1080/01431160600746456

Lu, Y., Coops, N. C., & Hermosilla, T. (2017). Estimating urban vegetation fraction across 25 cities in pan-Pacific using Landsat time series data. ISPRS Journal of Photogrammetry and Remote Sensing, 126, 11–23. https://doi.org/10.1016/j.isprsjprs.2016.12.014

Ludwig, C., Hecht, R., Lautenbach, S., Schorcht, M., & Zipf, A. (2021). Mapping Public Urban Green Spaces Based on OpenStreetMap and Sentinel-2 Imagery Using Belief Functions. *ISPRS International Journal of Geo-Information*, *10*(4), 251. https://doi.org/10.3390/ijgi10040251

Madureira, H., & Andresen, T. (2013). Planning for multifunctional urban green infrastructures: Promises and challenges. *URBAN DESIGN International*, *19*(1), 38–49. https://doi.org/10.1057/udi.2013.11

Millennium Ecosystem Assessment, 2005. Ecosystems and Human Well-being: Synthesis. Island Press, Washington, DC. ISBN 1-59726-040-1

Ming, D., Li, J., Wang, J., & Zhang, M. (2015). Scale parameter selection by spatial statistics for GeOBIA: Using mean-shift based multi-scale segmentation as an example. *ISPRS Journal of Photogrammetry and Remote Sensing*, *106*, 28–41. https://doi.org/10.1016/j.isprsjprs.2015.04.010

Misiune, I., Julian, J. P., & Veteikis, D. (2021). Pull and push factors for use of urban green spaces and priorities for their ecosystem services: Case study of Vilnius, Lithuania. *Urban Forestry & Urban Greening*, *58*, 126899. https://doi.org/10.1016/j.ufug.2020.126899

Mountrakis, G., Im, J., & Ogole, C. (2011). Support vector machines in remote sensing: A review. *ISPRS Journal of Photogrammetry and Remote Sensing*, *66*(3), 247–259. https://doi.org/10.1016/j.isprsjprs.2010.11.001

Neyns, R., & Canters, F. (2022). Mapping of Urban Vegetation with High-Resolution Remote Sensing: A Review. Remote Sensing, 14(4), 1031. https://doi.org/10.3390/rs14041031

Niculescu, S., & Lam, C. N. (2019). Geographic Object-Based Image Analysis of Changes in Land Cover in the Coastal Zones of the Red River Delta (Vietnam). *Journal of Environmental Protection*, *10*(03), 413–430. https://doi.org/10.4236/jep.2019.103024

Noszczyk, T., Gorzelany, J., Kukulska-Kozieł, A., & Hernik, J. (2022). The impact of the COVID-19 pandemic on the importance of urban green spaces to the public. *Land Use Policy*, *113*, 105925. https://doi.org/10.1016/j.landusepol.2021.105925

OpenStreetMap Wiki (2022). About OpenStreetMap. https://wiki.openstreetmap.org/wiki/About_OpenStreetMap

Ozlem Yilmaz, E., Varol, B., Hale Topaloglu, R., & Sertel, E. (2019). Object-Based Classification of Izmir Metropolitan City by Using Sentinel-2 Images. *2019 9th International Conference on Recent Advances in Space Technologies (RAST)*. https://doi.org/10.1109/rast.2019.8767781

Pandey, P. C., N. Koutsias, G.P. Petropoulos, P.K. Srivastava & E.B. Dor (2019): Land Use/Land Cover in view of Earth Observation: Data Sources, Input Dimensions and Classifiers -a Review of the State of the Art". Geocarto International, [in press]

Pandey, P.C., P.K. Srivastava, H. Baltzer, B. Bhattacgarya & G.P. Petropoulos (2020): Hyperspectral Remote Sensing: Theory & Applications. Elsevier, ISBN: 978-0-08-102894-0

Pappas, V. (2017). Γεωγραφικά Συστήματα Πληροφοριών και Σχεδιασμός του Χώρου. [Geographic Information Systems and Spatial Planning]. Pp 11-14. University of Patras Publications. Pp 11-14. ISBN 978-960-530-116-3

Parcharidis, I. (2015). Αρχές δορυφορικής τηλεπισκόπησης [Undergraduate textbook]. [Principles of satellite remote sensing]. Kallipos, Open Academic Editions. http://hdl.handle.net/11419/3960

Perakis, K., Moysiadis, A., & Faraslis, I. (2015). Η τηλεπισκόπηση σε 13 ενότητες [Undergraduate textbook]. [Remote sensing in 13 sections]. Kallipos, Open Academic Editions. http://hdl.handle.net/11419/1840

Petropoulos, G. P., Arvanitis, K., & Sigrimis, N. (2012). Hyperion hyperspectral imagery analysis combined with machine learning classifiers for land use/cover mapping. *Expert Systems with Applications*, *39*(3), 3800–3809. https://doi.org/10.1016/j.eswa.2011.09.083

Petropoulos, G. P., Kalaitzidis, C., & Prasad Vadrevu, K. (2012). Support vector machines and object-based classification for obtaining land-use/cover cartography from Hyperion hyperspectral imagery. *Computers & Geosciences*, *41*, 99–107. https://doi.org/10.1016/j.cageo.2011.08.019

Petropoulos, G. P., Kalivas, D. P., Georgopoulou, I. A., & Srivastava, P. K. (2015). Urban vegetation cover extraction from hyperspectral imagery and geographic information system spatial analysis techniques: case of Athens, Greece. *Journal of Applied Remote Sensing*, *9*(1), 096088. https://doi.org/10.1117/1.jrs.9.096088

Petropoulos, G. P., Kontoes, C. C., & Keramitsoglou, I. (2012). Land cover mapping with emphasis to burnt area delineation using co-orbital ALI and Landsat TM imagery. *International Journal of Applied Earth Observation and Geoinformation*, *18*, 344–355. https://doi.org/10.1016/j.jag.2012.02.004

Petropoulos, G. P., Partsinevelos, P., & Mitraka, Z. (2013). Change detection of surface mining activity and reclamation based on a machine learning approach of multi-temporal Landsat TM imagery. *Geocarto International*, *28*(4), 323–342. https://doi.org/10.1080/10106049.2012.706648

Petropoulos, G. P., Vadrevu, K. P., & Kalaitzidis, C. (2013). Spectral angle mapper and object-based classification combined with hyperspectral remote sensing imagery for obtaining land use/cover mapping in a Mediterranean region. *Geocarto International*, *28*(2), 114–129. https://doi.org/10.1080/10106049.2012.668950

Pinto, L., Ferreira, C. S., & Pereira, P. (2021). Environmental and socioeconomic factors influencing the use of urban green spaces in Coimbra (Portugal). *Science of The Total Environment*, *792*, 148293. https://doi.org/10.1016/j.scitotenv.2021.148293

Planet (2021). Planet Imagery Product Specifications. https://assets.planet.com/docs/Planet_Combined_Imagery_Product_Specs_letter_screen.pdf

Planet (2022). Understanding PlanetScope Instruments. (2022). https://developers.planet.com/docs/apis/data/sensors/

Planet Explorer (2021). Planet. https://www.planet.com/explorer/

Puissant, A., Rougier, S., & Stumpf, A. (2014). Object-oriented mapping of urban trees using Random Forest classifiers. *International Journal of Applied Earth Observation and Geoinformation*, *26*, 235–245. https://doi.org/10.1016/j.jag.2013.07.002

Puplampu, D. A., & Boafo, Y. A. (2021). Exploring the impacts of urban expansion on green spaces availability and delivery of ecosystem services in the Accra metropolis. *Environmental Challenges*, *5*, 100283. https://doi.org/10.1016/j.envc.2021.100283

Reyes-Riveros, R., Altamirano, A., de la Barrera, F., Rozas-Vásquez, D., Vieli, L., & Meli, P. (2021). Linking public urban green spaces and human well-being: A systematic review. *Urban Forestry & Urban Greening*, *61*, 127105. https://doi.org/10.1016/j.ufug.2021.127105

Scott, D., Petropoulos, G., Moxley, J., & Malcolm, H. (2014). Quantifying the Physical Composition of Urban Morphology throughout Wales Based on the Time Series (1989–2011) Analysis of Landsat TM/ETM+ Images and Supporting GIS Data. *Remote Sensing*, *6*(12), 11731–11752. https://doi.org/10.3390/rs61211731

Segment Mean Shift (Image Analyst)—ArcGIS Pro | Documentation. (2022). ESRI. https://pro.arcgis.com/en/pro-app/latest/tool-reference/image-analyst/segment-mean-shift.htm

Selmi, W., Weber, C., Rivière, E., Blond, N., Mehdi, L., & Nowak, D. (2016). Air pollution removal by trees in public green spaces in Strasbourg city, France. *Urban Forestry & Urban Greening*, *17*, 192–201. https://doi.org/10.1016/j.ufug.2016.04.010

Sentinel-2 Specifications (2022). Sentinel Online. European Space Agency. https://sentinel.esa.int/web/sentinel/missions/sentinel-2

Shahtahmassebi, A. R., Li, C., Fan, Y., Wu, Y., Lin, Y., Gan, M., Wang, K., Malik, A., & Blackburn, G. A. (2021). Remote sensing of urban green spaces: A review. Urban Forestry & Urban Greening, 57, 126946. https://doi.org/10.1016/j.ufug.2020.126946

Shao, Y., & Lan, J. (2019). A Spectral Unmixing Method by Maximum Margin Criterion and Derivative Weights to Address Spectral Variability in Hyperspectral Imagery. Remote Sensing, 11(9), 1045. https://doi.org/10.3390/rs11091045

Sharifi, F., Nygaard, A., Stone, W. M., & Levin, I. (2021). Accessing green space in Melbourne: Measuring inequity and household mobility. Landscape and Urban Planning, 207, 104004. https://doi.org/10.1016/j.landurbplan.2020.104004

Shekhar, S., & Aryal, J. (2019). Role of geospatial technology in understanding urban green space of Kalaburagi city for sustainable planning. Urban Forestry & Urban Greening, 46, 126450. https://doi.org/10.1016/j.ufug.2019.126450

Sheykhmousa, M., Mahdianpari, M., Ghanbari, H., Mohammadimanesh, F., Ghamisi, P., & Homayouni, S. (2020). Support Vector Machine Versus Random Forest for Remote Sensing Image Classification: A Meta-Analysis and Systematic Review. IEEE Journal of Selected Topics in Applied Earth Observations and Remote Sensing, 13, 6308–6325. https://doi.org/10.1109/jstars.2020.3026724

Simionato, J., Bertani, G., & Osako, L. S. (2021). Identification of artisanal mining sites in the Amazon Rainforest using Geographic Object-Based Image Analysis (GEOBIA) and Data Mining techniques. *Remote Sensing Applications: Society and Environment*, *24*, 100633. https://doi.org/10.1016/j.rsase.2021.100633

Souza-Filho, P., Nascimento, W., Santos, D., Weber, E., Silva, R., & Siqueira, J. (2018). A GEOBIA Approach for Multitemporal Land-Cover and Land-Use Change Analysis in a Tropical Watershed in the Southeastern Amazon. *Remote Sensing*, *10*(11), 1683. https://doi.org/10.3390/rs10111683

Timilsina, S., Aryal, J., & Kirkpatrick, J. B. (2020). Mapping Urban Tree Cover Changes Using Object-Based Convolution Neural Network (OB-CNN). *Remote Sensing*, *12*(18), 3017. https://doi.org/10.3390/rs12183017

Topaloğlu, R. H., Aksu, G. A., Ghale, Y. A. G., & Sertel, E. (2021). High-resolution land use and land cover change analysis using GEOBIA and landscape metrics: A case of Istanbul, Turkey. *Geocarto International*, 1–27. https://doi.org/10.1080/10106049.2021.2012273

Train Random Trees Classifier (Image Analyst)—ArcGIS Pro | Documentation. (2022). ESRI. https://pro.arcgis.com/en/pro-app/latest/tool-reference/image-analyst/train-random-trees-classifier.htm

Understanding PlanetScope Instruments. (2022). Planet. https://developers.planet.com/docs/apis/data/sensors/

United Nation, Department of Economic and Social Affairs, & Population Division. (2018). World urbanization prospects: The 2018 Revision – key facts.

Urban Green (2020). World Wide Fund Greece. https://www.wwf.gr/ti_kanoume/anthropos/astiko_prasino/

van der Schriek, T., Varotsos, K. V., Giannakopoulos, C., & Founda, D. (2020). Projected Future Temporal Trends of Two Different Urban Heat Islands in Athens (Greece) under Three Climate Change Scenarios: A Statistical Approach. *Atmosphere*, *11*(6), 637. https://doi.org/10.3390/atmos11060637

Vargas-Munoz, J. E., Srivastava, S., Tuia, D., & Falcao, A. X. (2021). OpenStreetMap: Challenges and Opportunities in Machine Learning and Remote Sensing. *IEEE Geoscience and Remote Sensing Magazine*, *9*(1), 184–199. https://doi.org/10.1109/mgrs.2020.2994107

Wang, J., Zhou, W., Pickett, S. T., Yu, W., & Li, W. (2019). A multiscale analysis of urbanization effects on ecosystem services supply in an urban megaregion. *Science of The Total Environment*, *662*, 824–833. https://doi.org/10.1016/j.scitotenv.2019.01.260

Whyte, A., Ferentinos, K. P., & Petropoulos, G. P. (2018). A new synergistic approach for monitoring wetlands using Sentinels -1 and 2 data with object-based machine learning algorithms. *Environmental Modelling & Software*, *104*, 40–54. https://doi.org/10.1016/j.envsoft.2018.01.023

Wicaksono, P., & Aryaguna, P. A. (2020). Analyses of inter-class spectral separability and classification accuracy of benthic habitat mapping using multispectral image. Remote Sensing Applications: Society and Environment, 19, 100335. https://doi.org/10.1016/j.rsase.2020.100335

Wulder, M. A., Coops, N. C., Roy, D. P., White, J. C., & Hermosilla, T. (2018). Land cover 2.0. *International Journal of Remote Sensing*, *39*(12), 4254–4284. https://doi.org/10.1080/01431161.2018.1452075

Wüstemann, H., Kalisch, D., & Kolbe, J. (2017). Access to urban green space and environmental inequalities in Germany. *Landscape and Urban Planning*, *164*, 124–131. https://doi.org/10.1016/j.landurbplan.2017.04.002

Zhou, L., Tian, Y., Myneni, R. B., Ciais, P., Saatchi, S., Liu, Y. Y., Piao, S., Chen, H., Vermote, E. F., Song, C., & Hwang, T. (2014). Widespread decline of Congo rainforest greenness in the past decade. *Nature*, *509*(7498), 86–90. https://doi.org/10.1038/nature13265

Zylshal, Sulma, S., Yulianto, F., Nugroho, J. T., & Sofan, P. (2016). A support vector machine object based image analysis approach on urban green space extraction using Pleiades-1A imagery. *Modeling Earth Systems and Environment*, *2*(2). https://doi.org/10.1007/s40808-016-0108-8